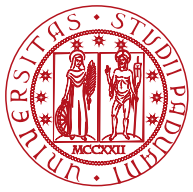

UNIVERSITÀ
DEGLI STUDI
DI PADOVA

DIPARTIMENTO DI INGEGNERIA INDUSTRIALE

TESI DI LAUREA MAGISTRALE IN
INGEGNERIA ENERGETICA

AIR INJECTION IN THE DRAFT TUBE OF A FRANCIS TURBINE TO IMPROVE THE EFFICIENCY: A SPERIMENTAL STUDY.

RELATORE: Prof. Anna Stoppato

CORRELATORI: Prof. Torbjorn K. Nielsen, Prof. Michel Cervantes

LAUREANDO: Alberto Marzotto

ANNO ACCADEMICO 2014-15

This thesis is realized in collaboration with:

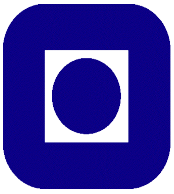

NTNU
Norwegian University of
Science and Technology

Ringraziamenti

Questa tesi è il coronamento di un lungo percorso di studi, che ha alternato momenti belli a momenti più difficili. Sarebbe stato impossibile per me arrivare fino a questo punto senza l'appoggio di alcune persone molto importanti per me, che desidero ringraziare.

Innanzitutto, mio padre e mia madre, che mi hanno sempre supportato nei momenti difficili, credendo nelle mie potenzialità e dandomi tutto il loro amore e appoggio.

Mi sembra giusto ringraziare anche tutti i miei amici, quelli del "Garage" e della biblioteca, per avermi sopportato durante i periodi di nervosismo tirandomi su di morale quando le cose non andavano, supportandomi e sopportandomi, quelli dell'università, per avermi aiutato a raggiungere questo traguardo, e quelli del calcio, che mi sono sempre stati accanto.

Desidero inoltre ringraziare la Professoressa Anna Stoppato e il Professor Torbjorn K. Nielsen, per avermi dato l'opportunità di svolgere questa tesi in Norvegia. Una menzione va anche a Michel Cervantes, che mi ha seguito durante tutto il lavoro in laboratorio, sempre con entusiasmo, e ad Alessandro Nocente e a Chirag Trivedi per il loro aiuto.

Volevo inoltre ringraziare Francesca, per essermi sempre stata accanto.

Sommario

Lo scopo di questa tesi è studiare il comportamento delle bolle iniettate nel tubo di scarico di una turbina Francis e la possibilità di utilizzare questo metodo per ridurre l'attrito tra l'acqua scaricata dalla turbina e la parete del tubo. La prima parte della tesi studia l'effettiva possibilità di utilizzare aria per ridurre l'attrito nel tubo di scarico, con calcoli e considerazioni basate sulla turbina Francis situata nel NTNU Water Power Laboratory. Per fare ciò, si è pensato di posizionare un anello tra la turbina e il tubo di scarico, con un numero di fori pari a 18500 e una portata di aria da iniettare calcolata in funzione della portata d'acqua in uscita dalla turbina, tutto ciò deciso dopo un approfondimento in letteratura unito ad uno studio delle caratteristiche dell'impianto.

A causa del lungo tempo che la creazione di questo anello avrebbe preso, e anche al grande investimento che sarebbe occorso per costruire l'anello e posizionarlo nell'impianto, si è deciso di effettuare uno studio preliminare sul comportamento delle bolle iniettate nel tubo di scarico, per scoprire se le caratteristiche delle bolle potrebbero assicurare una riduzione dell'attrito. La turbina è stata fatta lavorare su tre punti di lavoro diversi, carico parziale, alto carico e punto di massima efficienza, con una portata d'aria variabile iniettata da un solo iniettore, inizialmente con un foro di diametro 1 mm, poi con uno da 2 mm di diametro. Il parametro più importante da misurare è la dimensione delle bolle, per sapere se hanno la dimensione giusta per stare vicino alla parete e assicurare riduzione dell'attrito pelle. Per studiare questo, sono state prese foto delle bolle durante l'esperimento ed il loro diametro è stato misurato e confrontato con un diametro previsto, ricavato dalla letteratura. Inoltre, alcune considerazioni sulla direzione delle bolle iniettate e la loro distanza dalla parete, scoperte durante l'esperimento, vengono riportate.

Abstract

This thesis wants to study the behavior of the bubbles injected in a draft tube of a Francis turbine and the possibility to use this method to reduce the skin friction between the water discharged by the turbine and the wall of the draft tube. The first part of the thesis focus on the possibility about using the skin friction in the draft tube, based on the turbine of NTNU Water Power Laboratory. To do that, a ring positioned between the turbine and the draft tube could be used, with a number of holes of about 18500 and the right air flow rate depending on the water flow rate, found out after some calculation derived by the literature review and the characteristics of the plant.

Because of the long time that the creation of this ring would take, and also the great cost that would have create this ring and the machining of the turbine, it was decided to do a preliminary study concerning the behavior of the bubbles injected in the draft tube, to find out if the bubble characteristics could assure a skin friction reduction. The turbine is made run at three different working points, part load, high load and best efficiency point, with a varying air flow rate injected by only one injector, that could have an hole of 1 mm or 2 mm diameter. The most important parameter is the dimension of the bubbles, to know if they have the right size to stay close to the wall and assure skin friction reduction. To study that, pictures of the bubbles were taken and the diameter measured and compared to an expected diameter found out from the literature review. Furthermore, some considerations about the direction of the bubbles injected and their distance from the wall, found out during the experiment, are reported.

Index

Symbols

A_{in}: inlet section area of draft tube [m^2]

C_d: downstream DO concentration

C_s: water surface DO concentration

C_0: upstream DO concentration

Cf_0: frictional resistance coefficient

D: air injector's hole diameter [m]

H: total head across the turbine [m]

H_p: head of the turbine [m]

H_0: head of the reservoir [m]

H_1: total height at the entrance of the turbine [m]

N_{QE}: dimensionless turbine's specific speed

P_a: pressure of the air [bar]

P_{a_std}: standard pressure of the air = 1 bar

P_{in}: pressure in the draft tube [Pa]

P_1: water pressure at the inlet of the turbine [Pa]

P_2: pressure at the outlet of the turbine (inlet of the draft tube) [Pa]

Q_a: injected air flow rate [m^3/s]

$Q_{a\text{-}1hole}$: air flow rate from one hole [m^3/s]

Q_p: discharge to the turbine [m^3/s]

Q_w: water flow rate passing through the turbine [m^3/s]

Re: Reynolds number

T_a: temperature of the air [K]

T_{a_std}: standard temperature of the air = 293.1 K

U_m : mean flow velocity [m/s]

U_w: water flow speed [m/s]

V_1: velocity of the water at the inlet of the turbine

V_2: velocity at the outlet of the turbine (inlet of the draft tube) [m/s]

V_3: fluid velocity leaving the draft tube [m/s]

Z: height of the turbine's inlet from the tail race [m]

d: air bubble's diameter [m]

d_{in}: inlet draft tube diameter [m]

d^*: non-dimensional bubble's diameter

e: dissolved oxygen efficiency

g: gravity acceleration = 9.81 m^2/s

h_{draft}: head losses in the draft tube [m]

h_f: lost due to the friction in the pipeline [m]

l_v: viscous length [m]

n: angular speed of the rotor [s^{-1}]

n_{holes}: number of holes

u^*: friction velocity [m/s]

α: void fraction

μ: dynamic viscosity [$kg/(m^2)$]

μ_0: dynamic water viscosity [$kg/(m^2)$]

η_{draft}: efficiency of the draft tube

ρ: density [kg/m^3]

ρ_a: density of the air [kg/m^3]

ρ_{a_std}: density of air at standard conditions = 1.293 kg/m^3

ρ_0: water density [kg/m^3]

τ: shear stress [Pa]

ν: kinematic viscosity [m^2/s]

ν_0: kinematic water viscosity [m^2/s]

Figures

Tables

1 Introduction

Hydropower is power derived from moving or falling water, and it is one of the best source of electricity on Earth. There are many benefits to use this source, because it is not a fossil fuel, so it does not product any greenhouse gases and other kind of water or air pollutant, and it is more predictable and controllable than wind or solar energy, because forecast tells about the rainfall and water is easy to collect. The diagram (Figure 1) shows perfectly the importance of hydropower, as the third source of energy for electricity generation, the most widely used among the renewables.

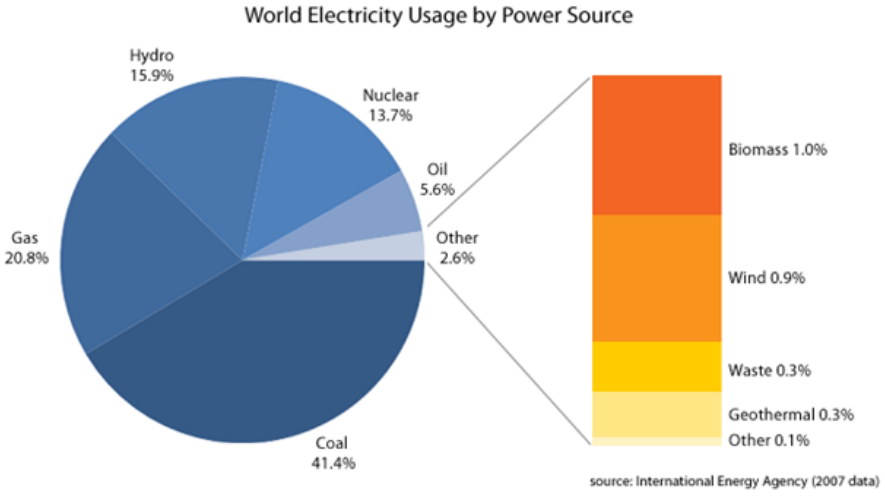

***Figure 1**- world electricity usage by power source.*

The world primary energy consumption is about 12730 Mtep (Primary energy demand), and a 6% of that is supply by hydropower, so it produces about 763.8 Mtep. The efficiency of a hydropower plant is about 90%, so also improve the efficiency of 1% could make an increase of the energy produced of about 8.5 Mtep.

The hydroelectric energy production has the benefit of not producing pollutant, dust and heat to discharge in the atmosphere, as opposed to other traditional thermoelectric generation methods. Focused on CO_2, the

emissions are reduced by 670 g per kWh of energy produced. So it has very important environmental advantages, but also some kind of disadvantages. One of them is the noise pollution, due mostly by the turbines, which can be reduced to values of 70 dB inside the station and almost zero outside it, so it is easily solved. Another one concerns the relationship with ecosystem, regarding the variation of the quantity of water in a river and the variation of the quality of the water. About the quantity of water, the plant has to guaranteed the vital minimum flow of water (DMV), which is the minimum water flow that has not to be used in the plant to assure the health of the ecosystem. Regarding the quality, when the water flows through the turbine of the plant, it loses some of the oxygen that is dissolved in it, which is very important for the health of the flora and fauna of the river. The plant has to guaranteed approved level of DO (Dissolved oxygen) of the water discharge in the river, that assure the health of the wildlife. Find a method to increase the DO level at the turbine discharge without affecting the efficiency of the turbine must be a purpose.

An hydraulic turbine could have an efficiency greater than 90%, which depends by the working point and the losses that are verified because the process could not be ideal. If the turbine is a reaction one, that means that it uses the pressure difference between inlet and discharge, to increase the efficiency an idea would be act on the draft tube by limiting the losses on it to have a greater pressure difference through the turbine. One way to do that is to inject air near the walls, so water meets less resistance going out from the turbine and waste less energy. Moreover, this method could increase the fraction of dissolved oxygen in water, with great benefits for the environment, and could be an efficient method to attenuate pressure fluctuations.

The first part of this thesis consists in a literature review of some of the most important articles and relations about air injection, concerning the

skin friction reduction, the increase of the dissolved oxygen in the water and a way to reduce the vibration of the turbines using air injection when they work at partial load. After that, there will be the theory chapter, divided in theory about the turbine, theory about air injection for skin friction reduction and theory about dissolved oxygen. About the turbine's subchapter, it is focalized more on the Francis turbine and its properties, especially concerning the draft tube, with a good explanation about how it works. The theory about air injection for skin friction reduction describes all the important parameters used in the study to find right amount of needed air. The last subchapter about dissolved oxygen talks about different methods to inject air for increase dissolved oxygen level in the water. Chapter 4 talks about the test rig and the presentation of the experiment, with a description about the turbine used on the experiment, the different working points studied and an explanation about what the experiment consist in. The materials and methods chapter shows and describe all the devices used to inject air in the draft tube. The final chapter resumes all the results of the experiment, with comments about them, and the conclusions, with some ideas for future developments and work that could be done.

2 Literature review

This section shows the main studies and findings regarding the air injection, in particular focused on the skin friction reduction, the increase of the dissolved oxygen in the water and as a method to reduce the vibration of the turbine when it works at part load.

2.1 Air injection and skin friction reduction

The use of air bubbles for the reduction of friction between a flow of water and a surface has been the subject of several studies in recent years. Some articles have focused on understanding the mechanism by which the friction reduction take places. L'vov et al. [1] tried to find a theory that describes how microbubbles can reduce the friction when their diameter is small enough to be not affected by gravity force, but only by Stokes force. Firstly, they found that we could use a one-fluid model also to describe the water flow with air in it, with density and viscosity that depend on the concentration of air in the water, as it is showed in formula 1 and formula 2:

$$\boldsymbol{\mu = \left(1 + \frac{5}{2}\alpha\right) * \mu_0} \qquad \textbf{Formula 1}$$

$$\boldsymbol{\rho = (1 - \alpha) * \rho_o} \qquad \textbf{Formula 2}$$

Where α is the void factor (concentration of air in the water), and μ_0 and ρ_0 are the dynamic viscosity and density of the water. After that, they focused on where put the bubbles to have the greatest drag reduction. When a fluid flows on plate, the velocity of this fluid is different close to the wall or away from it. It is possible to find three different regions, called layers, near the wall: the viscous layer, the buffer layer and the log-law region layer. To find the length of these layers, is better used the non-dimensional parameters y^+, called the wall coordinate:

$$y^+ = \frac{y * u^*}{\nu}$$ **Formula 3**

Where y is the distance from the wall, made unidimensional with u^*, which is the friction velocity, depending on the shear stress and the density of the fluid, and the kinematic viscosity of the fluid ν.

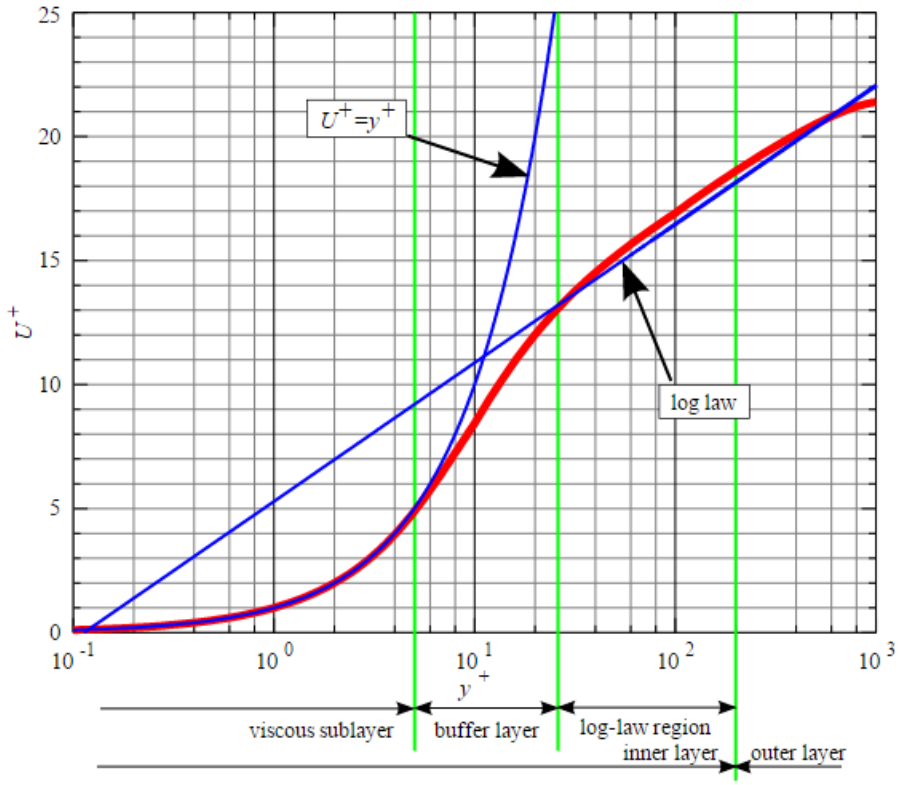

***Figure 2**- dimensionless velocity u^+ depending on different layer.*

Figure 2 shows how the dimensionless velocity u^+ vary depending on the different layer. This non-dimensional velocity is the velocity of the fluid depending on the distance from the wall y, divided by the friction velocity u^*. This study found that the best thing is to have the bubbles concentration outside the viscous layer, in the buffer layer, with $6 \leq y^+ \leq 30$.

Kato et al. [2] proposed some methods to control the size of the bubbles in a flat plate, testing different types of injectors with different flow velocities and air flow rate injected.

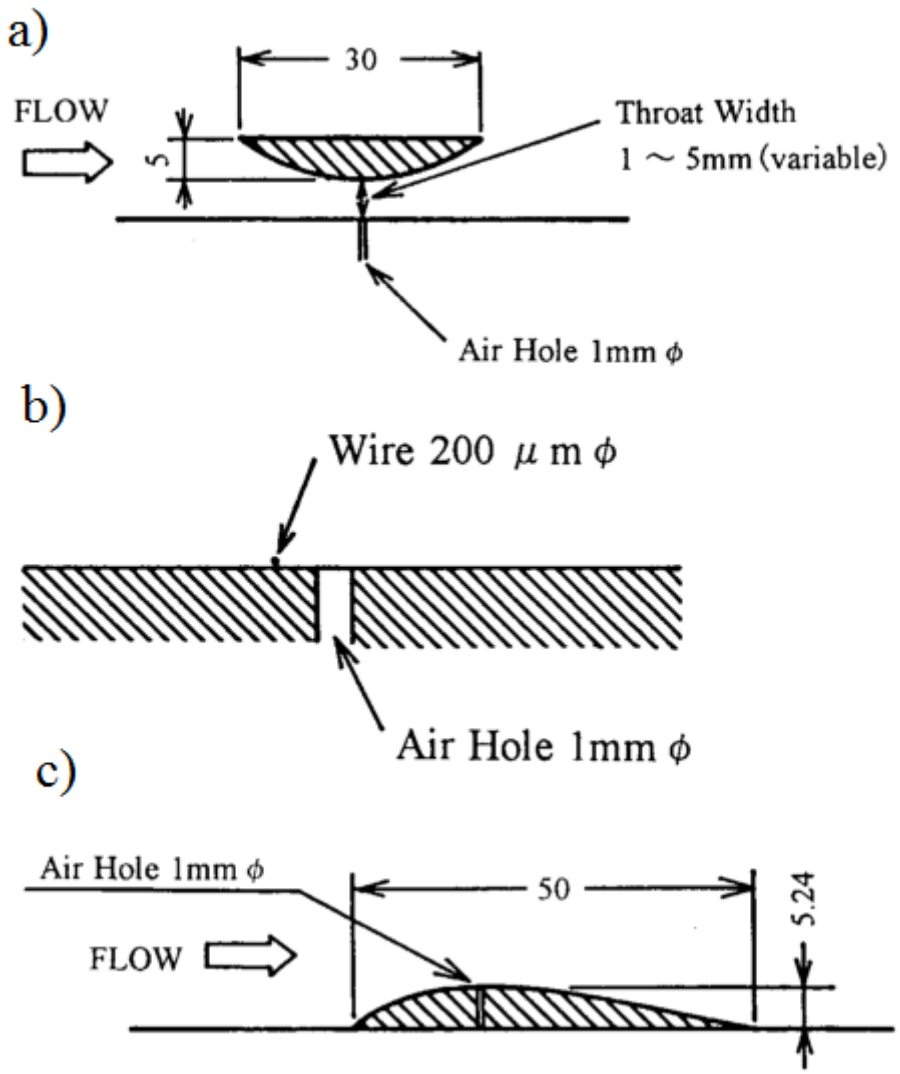

Figure 3*- 3 different methods for generate air bubbles: a) 2d convex shape, b) 2D convergent-divergent nozzle, c) little upstream of an ejection hole.*

Figure 3 shows the three different methods used for generate air bubbles, which are:

a) 2D convex shape with a 1mm injection hole's diameter at the top;
b) 2D convergent-divergent nozzle with an ejection hole of 1mm diameter at the throat and a transverse wire, with 0.2mm diameter;
c) Little upstream of an ejection hole of 1mm diameter.

They verified the relation:

$$\frac{d}{D} = 2.4 * (\frac{Q}{U * D^2})^2 \qquad \textbf{Formula 4}$$

among the bubbles diameter d and the diameter of injection hole D, the air flow rate Q and the water flow velocity U. They measured the size of the bubble using a film motion analyzer, with photographs take simultaneously from the top and the side of the injector.

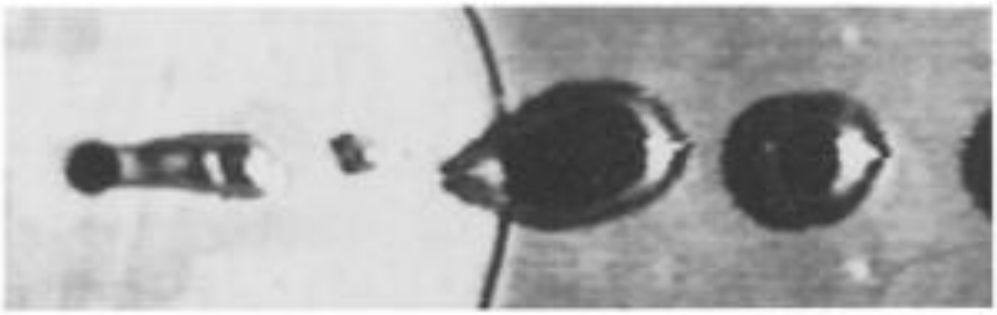

Figure 4*- picture of bubbles.*

Figure 4 shows a picture take from the top of the injector. They find that the 2D convex method is the best for create small bubbles and make a friction reduction. Moreover, they discovered that bubbles are very effective near the air injection point, but the effect rapidly decrease downstream.

Kato et al. [3] focalized more on the effect of microbubble diameter and distribution of microbubbles in the boundary layer, using a flat surface with a porous plate injector, changing air flow rate and water velocity. They found that skin friction was reduced of more than 40% with a void factor of 12% and that the highest is the water velocity, the smallest is diameter of microbubbles. In addition, they discovered that change of microbubbles diameter causes no change in frictional resistance. About that, very significant are the studies of Ceccio [4] and Shen et al. [5] both of them realized on a flat plate. The first compared many studies and discovered that injected bubbles with size ranging from $5 \leq d/l_v \leq 100$, where d is the diameter of the bubbles and l_v is the viscous length, don't

cause a significant change in drag reduction with the same void fraction. The second is an experiment where they change bubbles diameter by adding different type of surfactant to the water, with constant flow velocity and different air flow rate. They found that with a range of value of $d/l_v=200\div18$, the measured drag reduction has no significant changes. Therefore, for drag reduction is more influent where the bubbles are, instead of their size.

Many kinds of experiment try to use air injection system to improve efficiency, lot of them are in naval field. For example, Latorre et al. [6] used a 2.3 meter SES catamaran as a model, with 8 hull-side air injector and measured the skin friction reduction varying the velocity and the void fraction near the surface, with coating surface and no-coating surface.

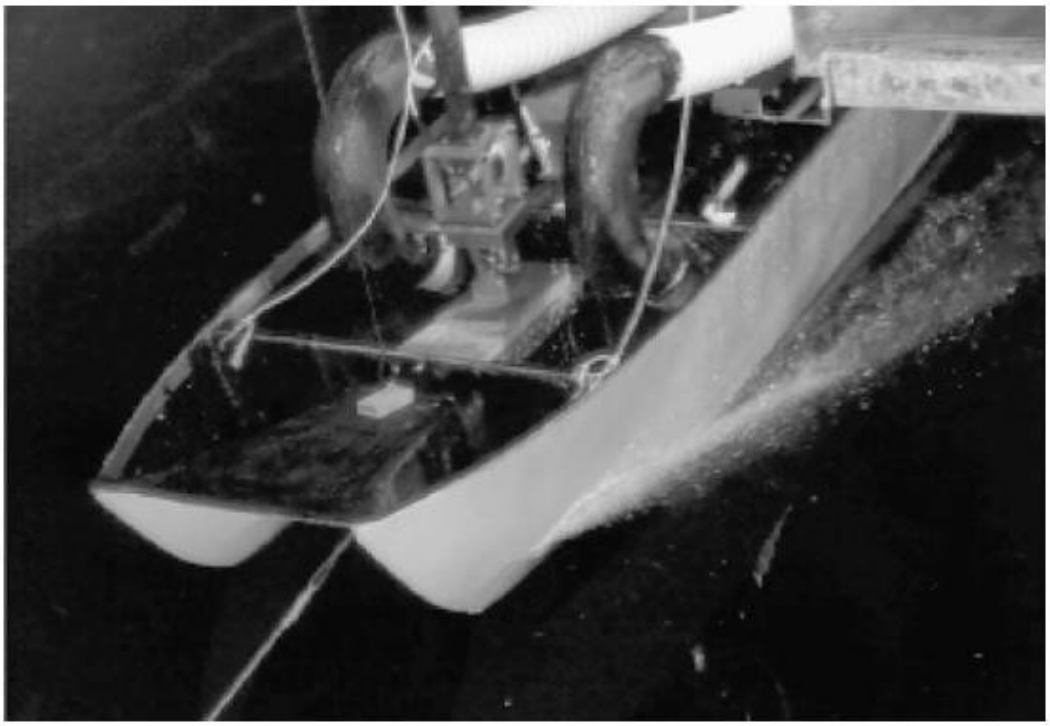

***Figure 5**- catamaran using air injection.*

Figure 5 shows the catamaran using air injectors. They found a drag reduction of about 5÷8% with no coating surface and 8÷11% with coating surface.

Several experiments used flat plate in circulating water tunnel to measure micro-bubble drag reduction (MBDR): Elbing et al. [7] studied the behavior of MBDR in a flat plate changing free-stream liquid velocity, gas flow rate injected and injector type. They saw that after 2 m from injector nearly total drag reduction was lost at higher flow speed and that there is a bubble-free liquid zone (called liquid layer) where bubbles do not reside. Moreover, they found that changes on injector geometry only had weak effect on effectiveness and downstream persistence of BDR. Kodama et al. [8] used a flat plate and a circulating water tunnel, changing the velocity of the flow and using a porous plate injector (Figure 6).

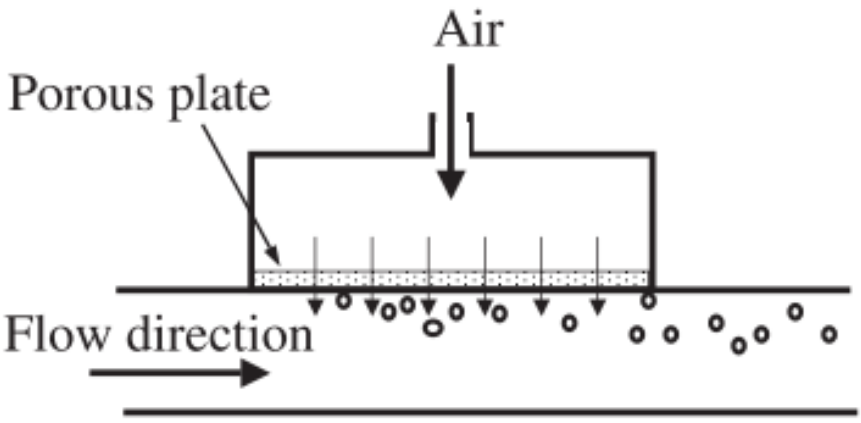

***Figure 6**- air injection by porous plate*.

They found that reduction of skin friction was greater at larger injection rate and lower speed and that is very important have the local void ratio close to the wall for skin friction reduction. Guin et al. [9] made experiment on a two-dimensional water channel with two porous plates (one on the top surface and one on the bottom surface of the channel) as injectors. This research discover that the bubbles need to stay close to the wall, in the buffer layer. Moreover, bubbles have no effect in reducing wall friction if they remain away from the wall by more than y^+=150 and the void fraction distribution for a given flow depends on its velocity and

the air flow rate. Sanders et al. [10] studied the skin friction reduction and some properties of it always in a flat plate in a circulating water channel with a high Reynold's number ($Re=210*10^6$), using a porous plate as injector. Like other studies, they found that bubbles have to stay close to the surface because the amount of drag reduction strongly depends on near-wall void fraction. In addition, they proved that bubbles tend to stay closer to the surface at higher injection rates for the same flow speed and injection locations, due to the skin friction decreases, and the friction reduction is lost when a liquid layer without bubble form on the surface of the plate.

Other experiments were taken on cylindrical device, that is more geometrical similar to a draft tube instead of a flat plate. About that, Nouri et al. [11] studied the skin friction reduction caused by injection of air in a rotational hub, varying the void fraction. In this case the air was injected direct with the water, as it is shown in figure 7.

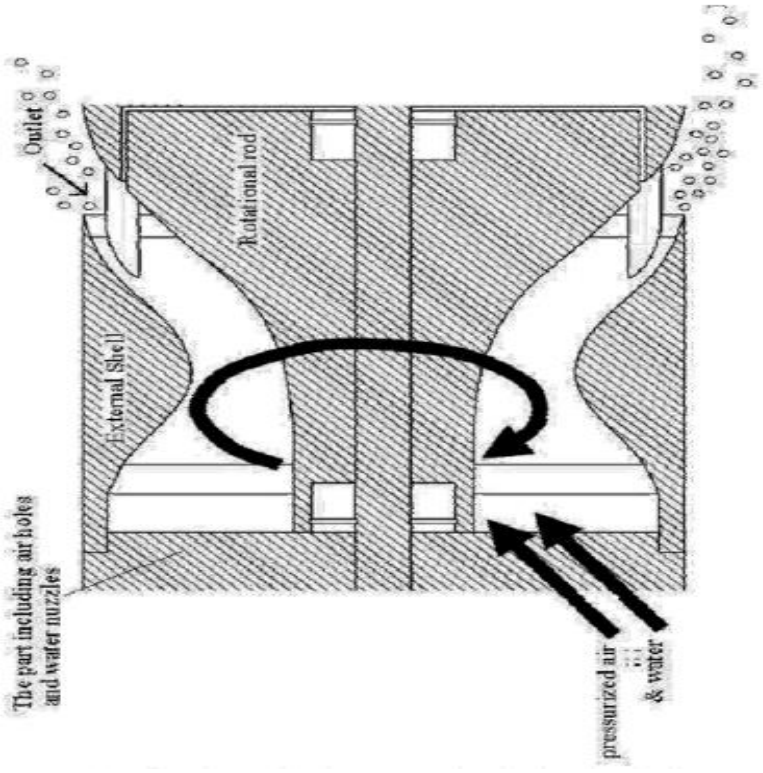

Figure 7*- air injection in a rotational rod.*

They found very good results, with friction reduction of 90% with a void fraction of about 3%. Van den Berg et al. [12] conducted similar experiment on a Taylor-Couette geometry to measure the effect of roughness on bubbly drag reduction. They found a strong drag reduction of about 25% when the void fraction is more than 2% in the smooth-wall case. Otherwise, in rough-wall case drag coefficient increased with void fraction, with a drag increase of 16% with a void fraction of 8%. The reason is that roughness destroy the smooth boundary layer, so the mechanism leading to bubble drag reduction.

At the end of this literature review, it is clear that injection of bubbles could be a great method to reduce the skin friction. About that, the most important thing to control is the distance of the bubble from the wall, that is regulate by the water flow velocity and the air injection flow rate, which also control the size of the bubbles.

2.2 Air injection and dissolved oxygen (DO)

The importance of Hydropower energy is due to the absence of emitted pollutant that makes this technology environmental friendly. One problem of the turbine concerning the environmental impact is the quality of the water that goes outside the turbine in the river. In fast-moving streams, rushing water is aerated by bubbles as it churns over rocks and falls down hundreds of tiny waterfalls. These streams, if unpolluted, are usually saturated with oxygen. In slow, stagnant waters, oxygen only enters the top layer of water, and deeper water is often low in DO concentration due to decomposition of organic matter by bacteria that live on or near the bottom of the reservoir. Moreover, the colder the water, the more oxygen can be dissolved in the water. Therefore, DO concentrations at one location are usually higher in the winter than in the summer. Hydroelectric

station used dams to made reservoir. If water is released from the top of the reservoir, it can be warmer because the dam has slowed the water, giving it more time to warm up and lose oxygen. If dams release water from the bottom of a reservoir, this water will be cooler, but may be low in DO due to decomposition of organic matter by bacteria.

About that, articles [13] and [14] are very interesting. The first one talks about the different quality of water in reference to the dissolved oxygen in it and some methods to improve it. It shows some existent methods to improve oxygen by injecting air in the draft tube, some results about dissolved oxygen in the water depending on how much air is injected, and in which position of the turbine is better to collocate injectors. The latter compares two kind of plate injectors, ceramic plate and metallic perforated plate (Figure 8: a) ceramic plate, b) metallic plate), to discover which one is the best, related not only to the mass transfer but also to the pressure drop.

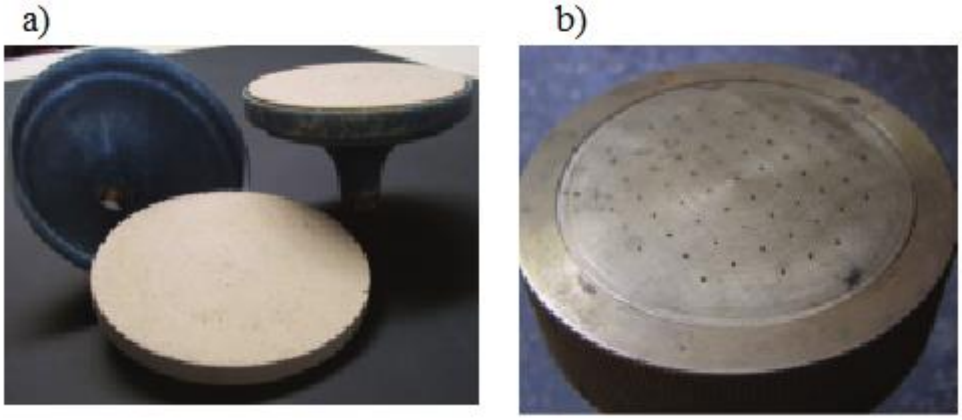

Figure 8*- example of plate injectors: a) ceramic plate, b) metallic plate.*

They find that metallic plates have the best oxygenation capacity with less pressure drop.

Papillon et al. [15] focalize on which position have to take the injectors to increase the dissolved oxygen. They make an experiment where they try

three kinds of runner cone venting and discharge ring aeration. They find that even if the runner cone has better capacity to inject air at almost every operating points, aeration by the discharge ring seems to favor oxygen transfer efficiency.

Very interesting is the study conducted by Principia Research Corporation [16], testing various method of increasing dissolved oxygen in a system operating. This research focalizes on determine the effect of air injection on the efficiency of generation unit and quantify the amount of air to inject over a range of turbine flow rates. Air is injected through holes on the runner, driven by the vacuum in the draft tube. They have an air-water flow ratio of 2.4% and see that at lower power outputs the addition of air improves efficiency, instead with high power outputs air admission causes a drop in efficiency. Moreover, with this ratio the dissolved oxygen increase is modest but measurable.

In the end, the low environmental impact is a very important characteristic of a plant, and the injection of air could be a perfect way to improve it, while preserving the ecosystem below the plant by increasing the dissolved oxygen in the water and therefore its quality. The challenge is to make it working with an improve or at least without change of the efficiency of the plant.

2.3 Air injection and vibration of the turbine at part load

When a Francis turbine operates off the point of maximum efficiency, usually at partial load, can occur a periodical fluctuation of water pressure, called surging phenomenon, which can lead to vibrate the draft tube, even to its breakage if the phenomenon is very accentuated. One method to decrease these vibrations could be air injection in the draft tube, which is the aim of Nakanishi et al. [17]. Their experiment consists in an “air pipe

test" using a model turbine under a high head, to have more energy of surging. Using that they want to find the operating conditions that causes the surging phenomenon, measure the best amount of air flow to decrease it and determine where to place air injectors.

They found that surging becomes stronger when guide vane opening was 60% of the guide vane opening at maximum efficiency. Moreover, they found that the optimum air flow rate is about 2% and the best position for air injectors is from 75% to 90% of the radius.

After that, it is clear that air supply in the draft tube could be very useful. It could improve the efficiency of the turbine, by reducing the skin friction of the water at the output so turbine has more pressure to elaborate, it could improve the dissolved oxygen, making the turbine more environmental friendly, and could prevent the surging phenomenon, avoiding damage at the power plant. The aim of this thesis is to prove the benefits of the air admission, injecting it in the draft tube of the Francis turbine situated in the NTNU Water Power Laboratory, varying the operation points, from partial load, to best efficiency load and high load, and varying the air flow rate.

3 Theory

To convert the mechanical energy of the water in electric energy a turbine has to be used. A turbine is a device consisting of a fixed portion, called stator, and a rotating part, called rotor, that is moved by the water flow and is connect to an electric generator to produce electricity. There are two types of turbine: impulse and reaction. The first type acts on a high velocity fluid to use its kinetic energy, used in case of high head (≥400 m) and low discharge. An example of this kind of turbine is Pelton. The latter type uses the pressure energy of the fluid to develop torque, used under low head (≤700 m) and high discharge. Examples of this kind of turbine are Francis and Kaplan.

3.1 Francis turbine

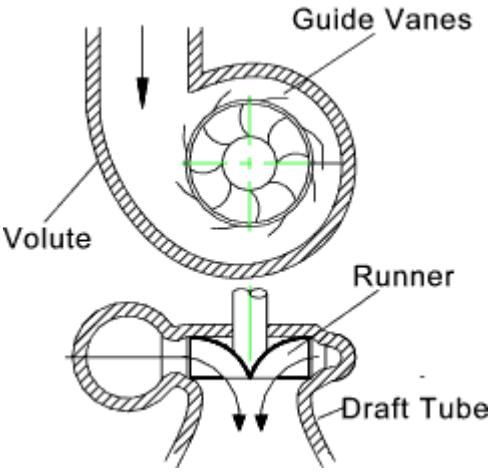

***Figure 9**- main part of a Francis turbine.*

Francis turbine is a reaction turbine and it is the most used for electric energy production. In this turbine, the water, which enters it, has to have high pressure. Part of the energy is given by the pressure change of the fluid passing through the blade, while the remaining portion is extracted by the volute part of the turbine. As can be seen from figure 9, a Francis turbine is composed by four main part: volute, guide vanes, runner and draft tube.

The volute consists in a spiral casing around the runner of the turbine. It has numerous openings that convert the pressure energy of the fluid in momentum energy before it interacts with the blades of the runner. To keep the flow constant, the cross sectional area of that device has to

decrease along the circumference. Guide vanes has to convert the pressure energy of the fluid in momentum energy and direct the flow at a right angle to the runner blades. The runner is the most important part of the turbine, because when the fluid impact with its blades create a tangential force which causes its rotation, that is transmitted to a generator, which produce electric energy. The crucial point is the inlet and outlet angles of the blade on the runner, because they are the most important parameters from which depends the power generation. The draft tube is a pipe that connects the exit of the turbine to the tail race where the fluid will be discharged. The main function of the draft tube is to convert the kinetic energy of the discharge water in other pressure energy used by the turbine. This is the part of the turbine where this thesis is focalized, so a better explanation on how it works is needed.

3.1.1 Draft tube

The draft tube is a diffuser that connect the end of the turbine to the tail race, which convert the dynamic pressure into static pressure. In this way, the fluid discharge in the tail race is slowed down, so there is less waste of kinetic energy and the turbine has an increase of the effective head across it. A very important parameter is the angle between the walls of the tube, which has to be limited to 8 degree, to reduce the energy loss in the tube and prevent the flow separation from the wall. Figure 10 is an example scheme of a plant:

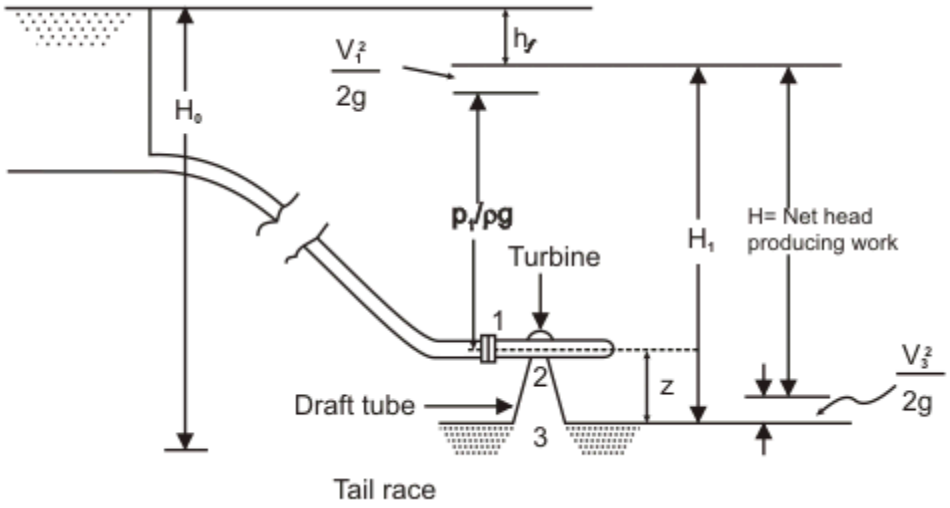

***Figure 10**- example scheme of a hydroelectric plant.*

The effective head across a turbine is the difference between the head at inlet and the head at outlet, so the inlet is the height of the reservoir, and the outlet is the tail race, because the draft tube connect turbine to it. Applying Bernoulli, the total height H_1 at the entrance of the turbine will be:

$$\boldsymbol{H_1 = H_0 - h_f = \frac{P_1}{\rho_0 g} + \frac{V_1^2}{2g} + z} \qquad \textbf{Formula 5}$$

The total head across the turbine H will be:

$$\boldsymbol{H = \frac{P_1}{\rho_0 g} + \frac{V_1^2}{2g} + z - \frac{V_3^2}{2g} = \left(H_0 - h_f\right) - \frac{V_3^2}{2g}}$$

Formula 6

If the losses in the draft tube are neglected, the head at the end of the turbine will be equal to the head at the discharge, so it means that:

$$\boldsymbol{\frac{P_2}{\rho_0 g} + \frac{V_2^2}{2g} + z = \frac{V_3^2}{2g}} \qquad \textbf{Formula 7}$$

$$\boldsymbol{\frac{P_2}{\rho_0 g} = -(z + \frac{V_2^2 - V_3^2}{2g})} \qquad \textbf{Formula 8}$$

Since $V_3<V_2$ and both terms are positive, it is possible to see that P_2 will be negative, and also z could be negative because of the reference height, which means that the turbine has the outlet section in depression, and recover more energy. It is possible to define the efficiency of the draft tube, η_{draft}, as the ratio of the difference between kinetic energy at inlet and outlet of the draft tube and the kinetic energy inlet:

$$\eta_{draft} = \frac{\left(V_2^2 - V_3^2\right) - 2gh_{draft}}{V_2^2} \qquad \textbf{Formula 9}$$

Therefore, the maximum conversion of kinetic energy in static energy, assuming no losses, would occur if the fluid came out of the draft tube with zero velocity. The problem is that the value of P_2 should not fall below the vapour pressure of the liquid, to avoid cavitation problem.

There are almost three different types of draft tube: the first one is called conical diffuser, and consists in a conic divergent used mostly for low specific speed, vertical shaft Francis turbine, with an efficiency η_{draft}=90% (Figure 11).

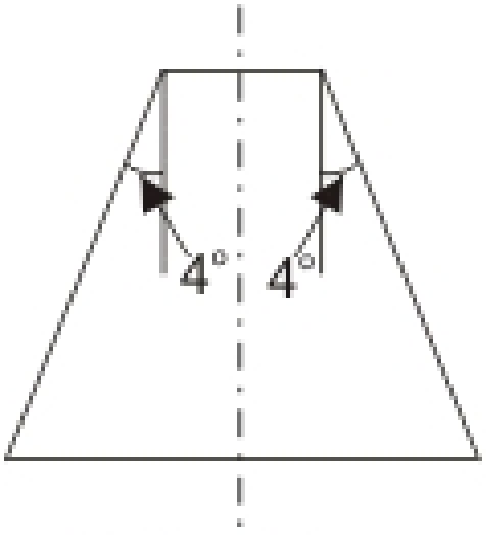

Figure 11*- conical diffuser draft tube.*

Another type is simple elbow draft tube, which is an extended elbow tube used mostly when the turbine is close to the tail race, with an efficiency η_{draft} less than 60% (Figure 12).

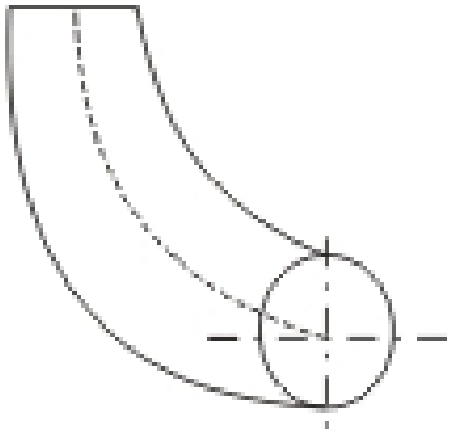

***Figure 12**- simple elbow draft tube.*

The last type is elbow with varying cross section, similar to the latter one except for the rectangular cross section at the outlet (Figure 13).

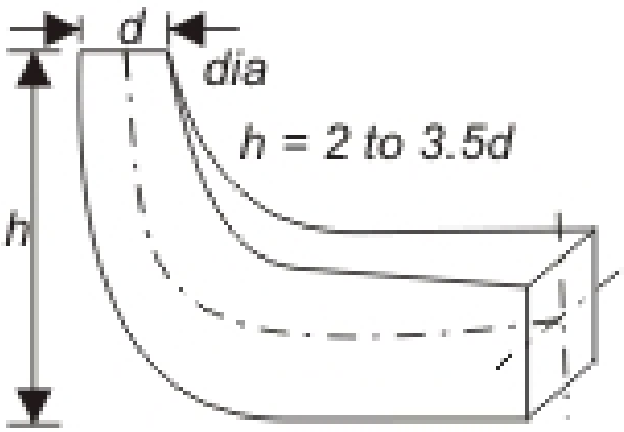

***Figure 13**- elbow with varying cross section draft tube.*

It is clear that the highest is the kinetic energy recovered with the draft tube the better is for the power generation. To improve that it is possible to act on the losses of the draft tube, that are caused by the friction of the liquid passing through it with the wall.

3.2 Air injection for skin friction reduction

One way to reduce the skin friction in the draft tube could be the injection of air near the wall. It is very important to know where is better to inject bubble and the size of the bubble that gives best results, and so understand better how this mechanism works.

The first parameter used to characterize air injection is the void fraction α, which indicates how much air is injected in the liquid:

$$\boldsymbol{\alpha = \frac{Q_a}{Q_a + Q_w}} \qquad \textbf{Formula 10}$$

Also with a very low value of that, less than 4%, is possible to obtain a friction reduction of about 90% [11]. The injection of air change the viscosity μ and the density ρ of the flow, but is still possible to consider the mixture like a one-model fluid described by:

$$\boldsymbol{\mu = \left(1 + \frac{5}{2}\alpha\right) * \mu_0} \qquad \textbf{Formula 1}$$

$$\boldsymbol{\rho = (1 - \alpha) * \rho_o} \qquad \textbf{Formula 2}$$

Where μ_0 and ρ_0 are the viscosity and the density of the water. These are not the only flow parameters that will change, another one will be the mean flow velocity U_m, which will be:

$$\boldsymbol{U_m = \frac{Q_a + Q_w}{A_{in}}} \qquad \textbf{Formula 11}$$

It is very useful to use non-dimensional parameter like S^+, z^+, W^+ and K^+, because it will be easier compare each other results from different studies:

$$\boldsymbol{S^+ = \left(\frac{\mu(z)}{p' * L}\right) * S} \qquad \textbf{Formula 12}$$

$$\boldsymbol{z^+ = z * \frac{\sqrt{\rho(z) * p' * L}}{\mu(z)}} \qquad \textbf{Formula 13}$$

$$W^+ = \frac{W}{p' * L}$$ **Formula 14**

$$K^+ = \frac{K}{p' * L}$$ **Formula 15**

Where μ is the viscosity, p' is the pressure gradient, L is the half channel width, S is the mean shear stress, z is the distance from the wall, ρ is the density, W is the Reynolds stress and K is the kinetic energy. With these parameters is possible to write the following balance equations:

$$S^+ + W^+ = 1$$ **Formula 16**

$$K^+ = c^2 * W^+$$ **Formula 17**

$$\left[\left(\frac{a}{z^+}\right)^2 + \frac{b}{z^+} * \sqrt{K^+}\right] * K^+ = W^+ * S^+$$ **Formula 18**

Where a and b are constant of the order of unit and c is a coefficient less or equal to 1.7. To have an indication about the effectiveness of this method, one way is to measure the difference of velocity of the flow with and without air injection, and that is what article [1] did, calculating the speed at a generic distance z from the wall in this way:

$$V(z) = \int_0^z S(z')dz' = \int_0^z \frac{p' * L}{\mu(z')} * S^+\left(z^+(z')\right)dz'$$

Formula 19

There is a drag reduction if the velocity with air bubbles is greater than the velocity with only water. The greatest drag reduction is obtained when the concentration of the air bubble is located outside the viscous layer, in the buffer layer, where $6 \leq z^+ \leq 30$.

One of the most useful relation is an experimental formula proved and used in [2]:

$$\frac{d}{D} = 2.4 * \left(\frac{Q_a}{U_w * D^2}\right)^{\frac{1}{2}} \qquad \textbf{Formula 20}$$

Since the diameter of the hole could be simplified, the size of the bubble is only function of the air and the water flow rate:

$$d = 2.4 * \left(\frac{Q_a}{U_w}\right)^{\frac{1}{2}} \qquad \textbf{Formula 21}$$

Another important parameter to know is the viscous length lv:

$$lv = \frac{v}{u^*} \qquad \textbf{Formula 22}$$

Where ν is the kinematic viscosity and u^* is the friction velocity, which is:

$$u^* = \sqrt{\frac{\tau}{\rho}} \qquad \textbf{Formula 23}$$

Where τ is the shear stress. With formula 21 and formula 22 it is possible to find the non-dimensional mean bubble diameter d^*:

$$d^* = \frac{d}{lv} \qquad \textbf{Formula 24}$$

This parameter is used in [4] and [5]: in both studies they change its value, in the first one the values are from 5 to 100, in the second one from 18 to 200, but not significant change in drag reduction were discovered. This means that the size of the bubbles does not directly influence the reduction of friction, but the gas volumetric flow rate which is in the boundary layer, controlled by free-stream pressure and injection rate, exerts most influence on drag reduction.

3.3 Air injection for dissolved oxygen

The dissolved oxygen (DO) is one of the parameters upon which depends the quality of the water going out from a hydropower plant. Depending on the value of DO, it is possible to classify different categories of water, in accordance with STAS 4706-88:

- 1st quality category: which could be drank or used by the food industry and for bathing or pools with a DO of about 6 mg/dm^3 ;
- 2nd quality category: which could be used for cleaning localities or for sailing or do aquatic sports with a DO of about 5 mg/dm^3;
- 3rd quality category: which could be used for industries, except food industries, and for agricultural irrigation system, with a DO of about 4 mg/dm^3.

A study done by Environmental Protection Agency (EPA) gives some minimum values of dissolved oxygen that permits the life of different species: for survival of trout DO has to be minimum 3 mg/l, for growth protection has to be 6.5 mg/l for an average of 30 days and for cold-water invertebrates has to be 4 mg/l.

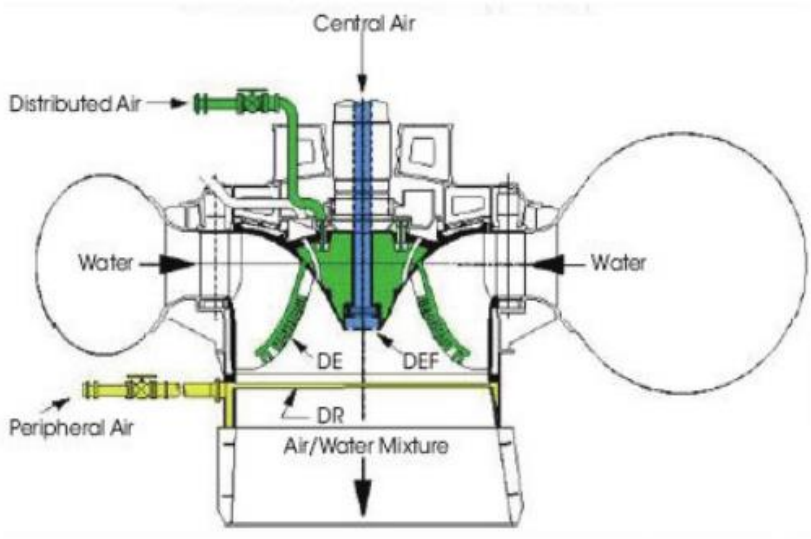

Figure 14*- 3 types of possible turbine aeration: central, peripheral and distributed.*

As it is shown in figure 14**,** there are 3 types of aeration for a turbine: central, peripheral and distributed. Different aeration system has different impact on the efficiency of the turbine, depending on the load of the turbine, as it is shown in [15].

About the dissolved oxygen efficiency, it is possible to express it in this way:

$$\boldsymbol{e = \frac{(C_d - C_0)}{(C_s - C_0)}} \qquad \textbf{Formula 25}$$

Where C_d, C_s and C_0 are the oxygen concentration respectively downstream, at the water surface and upstream. As is written in [13], injecting 1% of air flow rate compared to the water flow rate used, an increase of approximately 10% of the aeration efficiency is obtained, which depends on the gas-liquid contact area, the retention time and the temperature. Therefore, the solution is an aeration system, which creates a small bubble size, to increase contact area, which has also a minimum energy consumption, so very low pressure loss. About the pressure loss, the best solution, which comes out from [14] and [13], is to use metallic plates instead of ceramic, because of higher standard oxygen transfer rate with a lower pressure drop.

4 Test case and experiment

4.1 Test rig

All the laboratory tests and measurement have been collected from a model Francis turbine installed at NTNU's Water Power Laboratory (WPL) in Trondheim. The turbine is a 1:5.1 scale model of a real existing one, which operates at Tokke Power Plant in Norway. At the best efficiency point, the model produces a power of 0.03 MW. The length of runner outlet diameter is 0.319 m and the dimensionless specific speed of the turbine N_{QE} is 0.27, calculated using:

$$N_{QE} = \frac{2\pi n\sqrt{Q_P}}{(2gH_P)^{\frac{3}{4}}} \qquad \textbf{Formula 26}$$

During the experiment, the turbine will work at three different operating points, that are part load, best efficiency point (BEP) and high load. Main values of these operating points are well showed in table 1, taken by a previous study, called "Francis99", done on the same turbine [website 6]:

	Units	Symbol	Part Load	BEP	High Load
Net head	m	H	12.29	11.91	11.84
Flow rate	m^3/s	Q_w	0.071	0.203	0.221
Efficiency	%	η_M	71.69	92.61	90.66
Differential pressure	kPa	Δp	120.394	114.978	114.033
Density	kg/m^3	ρ_0	999.23	999.19	999.20
Kinematic viscosity	m^2/s	ν_0	$9.57*10^{-7}$	$9.57*10^{-7}$	$9.57*10^{-7}$
Dynamic viscosity	kg/(m*s)	μ_0	$9.56*10^{-4}$	$9.56*10^{-4}$	$9.56*10^{-4}$

***Table 1**- turbine's operating point values.*

Where the dynamic viscosity could be calculated using:

$$\boldsymbol{\mu_0 = \rho_0 * \upsilon_0} \qquad \textbf{Formula 27}$$

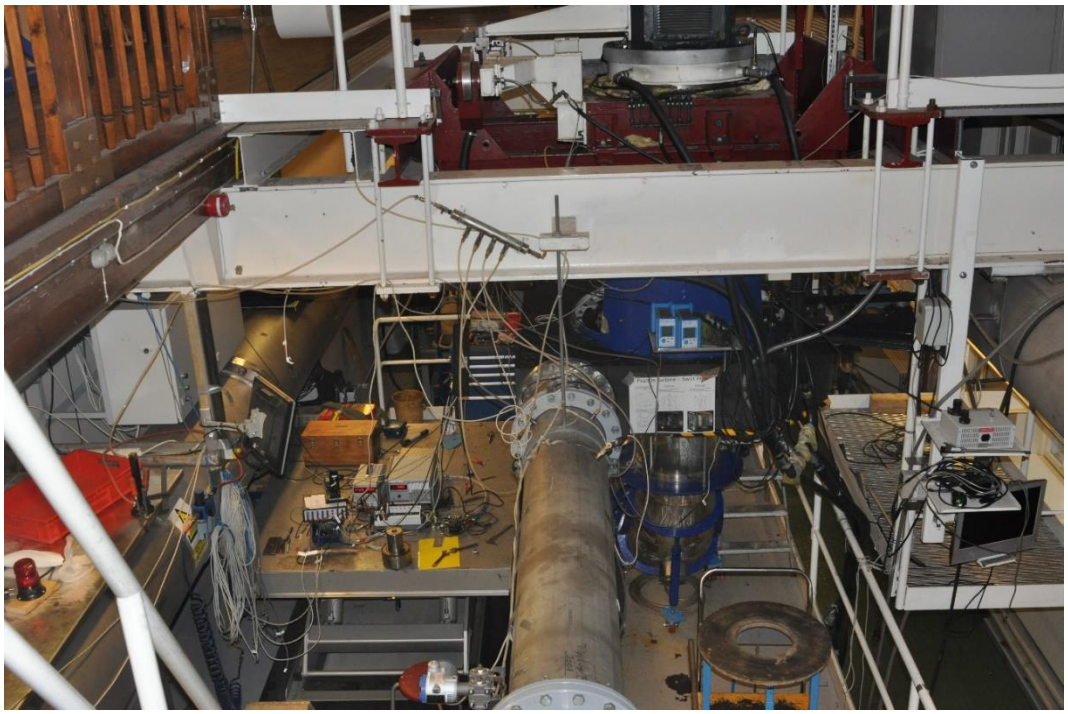

***Figure 15**- the NTNU's water power laboratory.*

A view of the Francis turbine is shown in figure 15, and a scheme of the test rig is shown in figure 16. The model is composed by an upstream pressure tank from which the water is taken and sent to the turbine. Between the tank and the pipeline there is a valve, which doesn't permit to vary continuously the water flow, but just close or open the circuit. In the pipeline, there are one magnetic flow meter measuring the water flow rate and two pressure transmitters (PTX1 and PTX2). After the second pressure transmitter there is the turbine, in which the water flow in the distributor, then in the runner and in the end in the draft tube, that is connected to the downstream tank. The guide vanes before the runner blades of the turbine's rotor, which are moved depending on the operating point choose, control the water flow. The runner of the turbine transmit the torque to the induction generator, which is connected using a vertical main shaft.

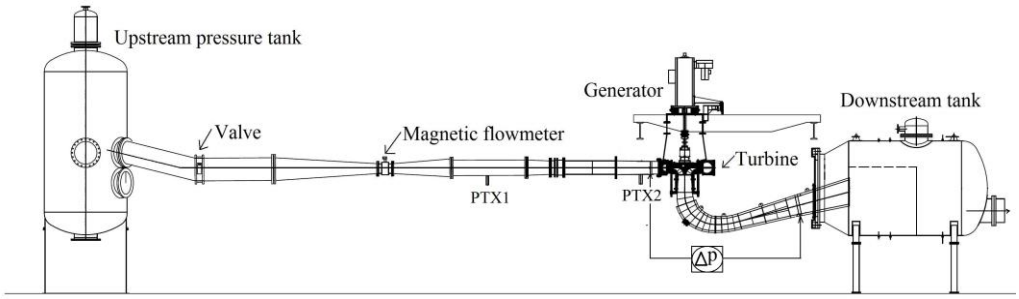

Figure 16*- test rig scheme.*

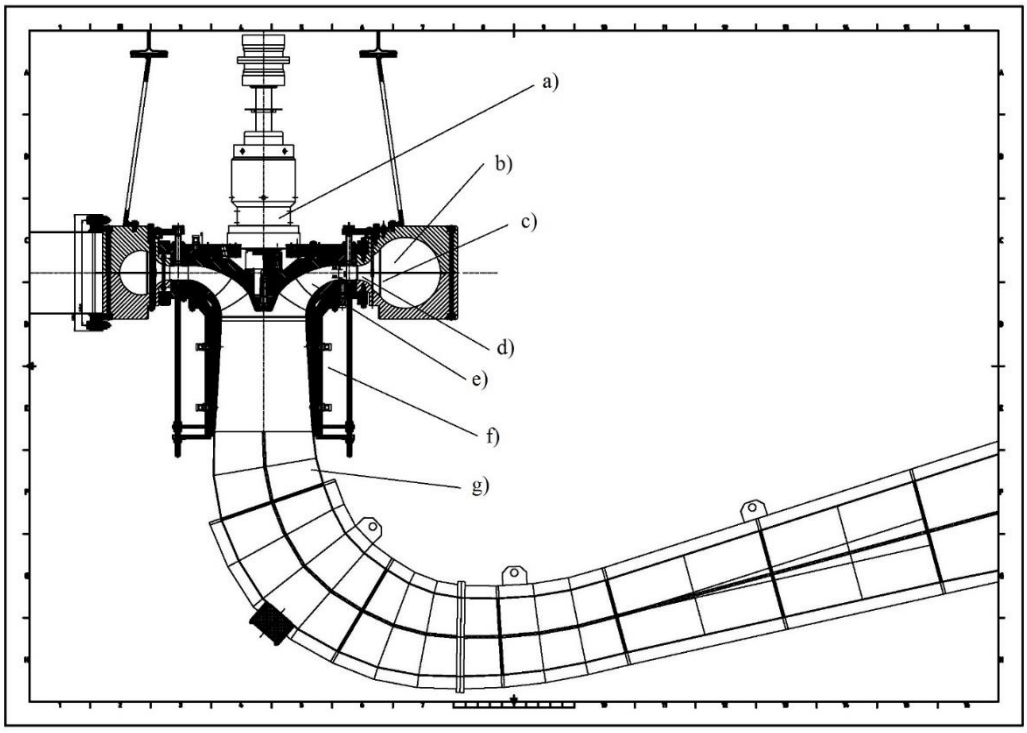

Figure 17*- scheme of the turbine: a) the thrust bearing, b) the spiral casing, c) stay vanes, d) guide vanes, e) runner, f) the cone draft tube, g) the draft tube.*

Figure 17 is focused more on the turbine and the draft tube. The first part of the draft tube is a plexiglass cone, which has an inlet internal diameter d_{in} of 0.35 m, is 0.48 m long and has an outlet diameter d_{out} of 0.40 m. The second part, which arrives to the downstream tank, is in stainless steel. With the inlet diameter and the water flow rate it is possible to calculate the velocity of the water U_w which comes out from the turbine, using:

$$U_w = \frac{Q_w}{A_{in}} = \frac{Q_w}{\pi * \frac{d_{in}^2}{4}} \qquad \textbf{Formula 28}$$

Depending on the different water flow rate, which depends on the operating points, the three water velocities are:

	Part Load	BEP	High Load
U_w [m/s]	0.74	2.11	2.30

With the water velocities, it is now possible to find the Reynolds number, that can be used for estimate if the flow in the draft tube is laminar or turbulent.

$$Re = \frac{U_w * d_{in}}{v_0} \qquad \textbf{Formula 29}$$

With the Reynolds number is possible to find also the frictional resistance coefficient Cf_0, using Formula 30 from [7], and with that is easy to obtain the shear stress τ using:

$$Cf_0 = 0.37 * (\log Re)^{-2.584} \qquad \textbf{Formula 30}$$

$$\tau = 0.5 * Cf_0 * \rho_0 * U_w^2 \qquad \textbf{Formula 31}$$

With the shear stress and the density, using formula 23 is possible to find the friction velocity, and after that the viscous length lv, with formula 22. All the results are shown in table 2:

	Part Load	BEP	High Load
Re	$2.70*10^{+5}$	$7.72*10^{+5}$	$8.40*10^{+5}$
Cf_0	$4.67*10^{-3}$	$3.79*10^{-3}$	$3.73*10^{-3}$
τ [kg/(m*s^2)]	1.27	8.43	9.83
u^* [m/s]	0.0357	0.0919	0.0992
lv	$2.68*10^{-5}$	$1.04*10^{-5}$	$9.56*10^{-5}$

***Table 2**- friction coefficient's value, with only water (no air injection).*

4.2 Experiment explanation

The experiment consists in driving the turbine at three different working point, which are part load, BEP and high load, and varying the injection of air on the draft tube, and so the void fraction, and see how the turbine reacts and works. The desired result is an improvement of the energy produced by the turbine, that has to be greater than the losses due to the air injection. To make continuous layer of bubbles all around the draft tube, the idea is to inject the air using a ring positioned between the output of the turbine and the beginning of the draft tube. As it is shown in the picture of the draft tube cone (Appendix A, Appendix B), the new ring would substitute the ring in the figure 18, which connects it to the turbine.

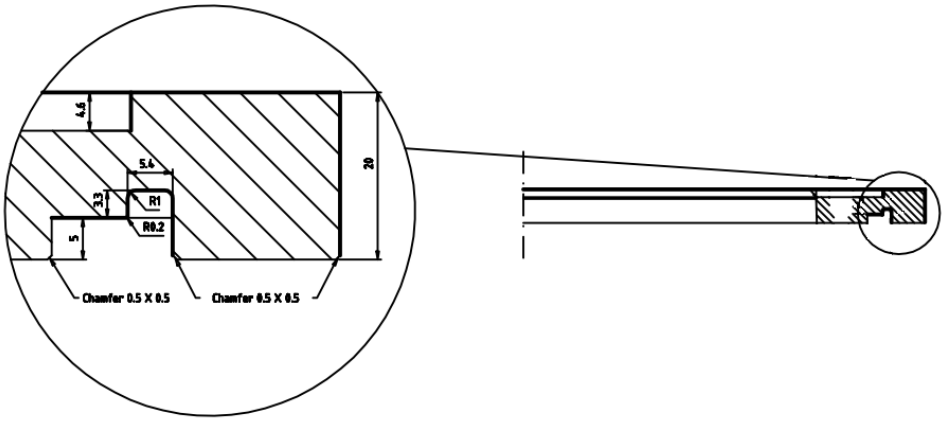

***Figure 18**- connection ring turbine-draft tube.*

The new ring has to have an inner and outer diameter as the first one, because the draft tube is the same, and a depth of the surface with holes that could vary from 5 mm to 15 mm, due to the overall dimensions of the connection between different parts.

So, the next step is understanding how much air has to be injected in the draft tube. Based on the literature review, it is clear that also with a small air flow rate a great friction reduction could be accomplished.

Each different operating point is tested with a void fraction α, calculated with formula 10, of 1%, 2% and 3%. The corresponding values of air flow rate Q_a are shown in table 3.

		α		
		1%	2%	3%
Q_a*10^{-4} (m^3/s)	Part Load	7.17	14.49	21.96
	BEP	20.51	41.43	62.78
	High Load	22.32	45.10	68.35

***Table 3**- air flow rate depending on operating point and void fraction.*

From the literature review, [4] and [5], it is possible to find the limits of the parameters d^*, which is related to the bubble size d using formula 22. These conditions are, for [4]: $5 \leq d^* \leq 100$, for [5]: $18 \leq d^* \leq 200$. These values are taken because bubbles with these dimensions assure the same skin friction reduction, so they stayed at the right distance from the wall, in the right layer. Using the lv values from table 2, is possible to find the value of the bubble's diameter.

For [4], so $5 \leq d^* \leq 100$:

	Minimum value [m]		Maximum value [m]
Part Load	$1.34 * 10^{-4}$	$\leq d \leq$	$2.68 * 10^{-3}$
BEP	$5.21 * 10^{-5}$	$\leq d \leq$	$1.04 * 10^{-3}$
High Load	$4.82 * 10^{-5}$	$\leq d \leq$	$9.65 * 10^{-4}$

***Table 4**- holes diameter's value using $5<d^*<100$.*

For [5], so $18 \leq d^* \leq 200$:

	Minimum value [m]		Maximum value [m]
Part Load	$4.83 * 10^{-4}$	≤ d ≤	$5.37 * 10^{-3}$
BEP	$1.88 * 10^{-4}$	≤ d ≤	$2.08 * 10^{-3}$
High Load	$1.74 * 10^{-4}$	≤ d ≤	$1.93 * 10^{-3}$

***Table 5**- holes diameter's value using $18<d^*<200$.*

The next step is to use a different version of formula 21. This formula permits to find the diameter of the bubbles created by one holes knowing the air flow rate and the velocity of the water. In the modified version, the total air flow rate is used, that depends on the void fraction, divided by the number of holes:

$$\boldsymbol{d = 2.4 * \left(\frac{Q_a}{n_{holes} * U_w}\right)^{\frac{1}{2}}} \qquad \textbf{Formula 32}$$

n_{holes}		Part Load			BEP			High Load	
	α	α	α	α	α	α	α	α	α
	1%	2%	3%	1%	2%	3%	1%	2%	3%
1000	2.37	3.36	4.14	2.37	3.36	4.14	2.37	3.36	4.14
5000	1.06	1.50	1.85	1.06	1.50	1.85	1.06	1.50	1.85
10000	0.75	1.06	1.31	0.75	1.06	1.31	0.75	1.06	1.31
15000	0.61	0.87	1.07	0.61	0.87	1.07	0.61	0.87	1.07
18000	0.56	0.79	0.98	0.56	0.79	0.98	0.56	0.79	0.98
18500	0.55	0.78	0.96	0.55	0.78	0.96	0.55	0.78	0.96

***Table 6**- attended bubble's diameters, depending on number of holes.*

In Table 6 the resulting bubbles diameter (in mm) using formula 32 are showed, with different number of holes and for all the operating points and void factors. The most restricted condition for the diameter range values is the one with $5 \leq d^* \leq 100$ from [4], which has the smallest maximum value of diameter permitted: it is easy to make a bubble with diameter greater than the minimum, instead is hard make a bubble with a smaller diameter than the maximum permitted. This condition will be the one taken for all next steps. All the diameters in the table are greater than the smallest permitted by the condition. So the hardest part is to find a number of holes which makee a diameter smaller than the maximum approved: to assure that, 18500 holes are needed.

After find the right number of holes which would make an ideal size of the bubbles, the next step is how to made this number of holes in the ring. Because of the impossibility to put one air injector for each hole due to

their big number, the idea consist in putting 24 injectors in the outer diameter, made a free material area inside the ring and then a thickness of porous material as inner surface. This would cause a difficulty regarding the determination of the actual number of holes and the type of material to be used. An easy way to solve this problem could consist in putting a thick weft net as inner surface. In this way is not so hard to find the number of holes and the problem is only find a net with the right weft, that assure at least 18500 holes (Figure 19).

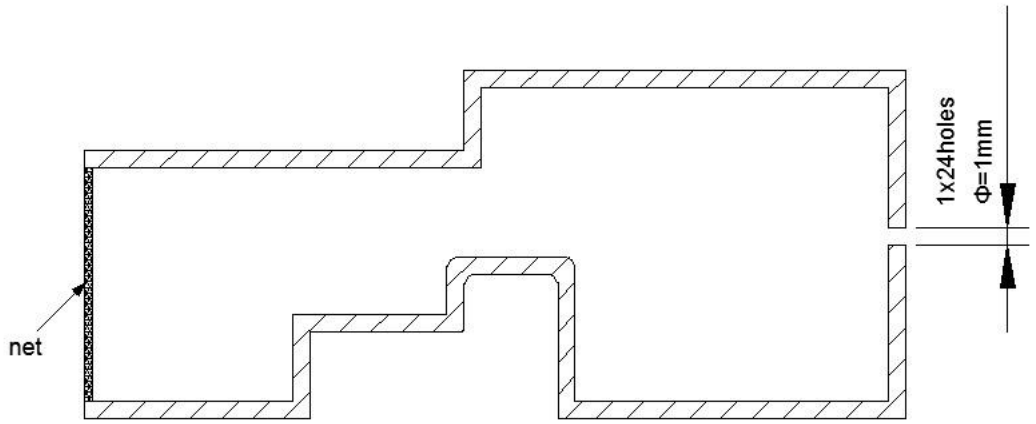

Figure 19*- example of ring injector using net.*

Because of the time that would take the production of this new ring and also the not negligible cost of this working (some tens of thousand euros), it is better to be more sure about the results of this. The idea is to inject air by only one hole, which is already present in the draft tube, also if not at ring height but at a distance of 11 cm from it, and watch the behavior of the bubbles (Figure 20).

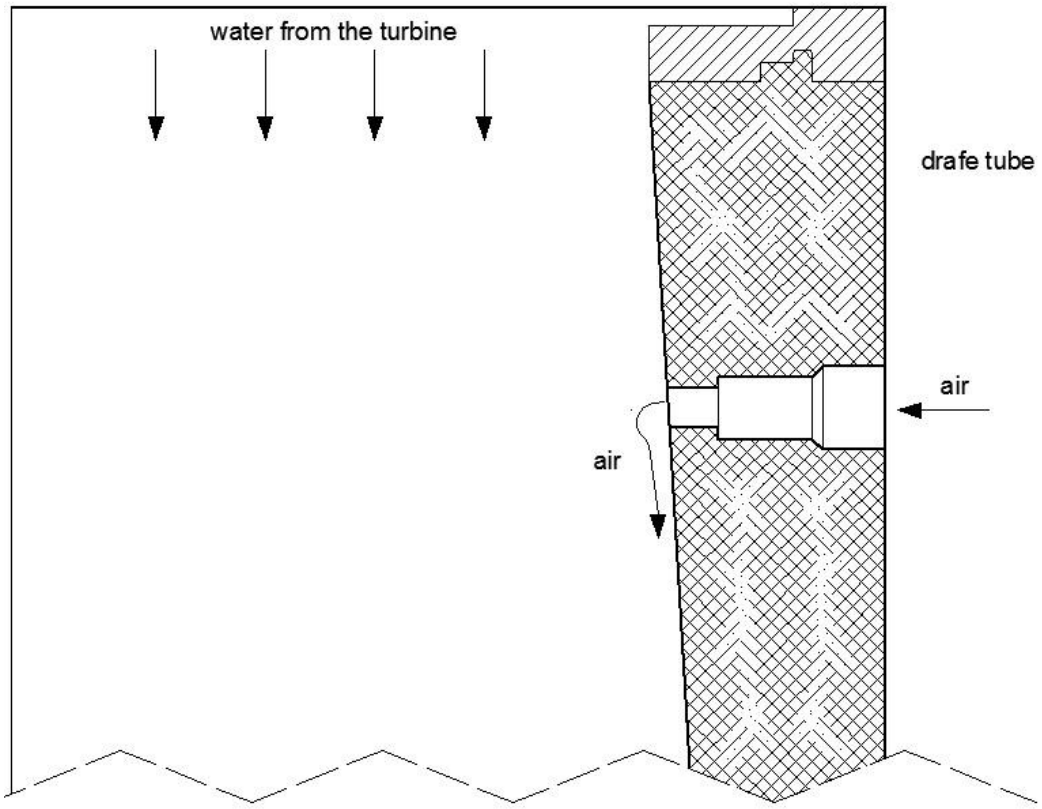

***Figure 20**- injection mechanism used in the experiment*.

Specifically, two kind of injectors have been used, one with a 1 mm diameter and one with 2 mm section, and different amount of air for every turbine's working points will be injected. The aim is to verify the accuracy of formula 21, and to see if bubbles stay close to the wall as expected.

The range of air flow rate that will be injected by the hole has to contain the value of air flow rate of a single hole of the hypothetic ring, calculate with this formula:

$$\boldsymbol{Q_{a-1hole} = \frac{Q_a}{n_{holes}}} \qquad \textbf{Formula 33}$$

Q_a varies depending on void fraction and working point, values are reported in table 3. The value of n_{holes} is 18500, found in table 6. The values of $Q_{a\text{-}1hole}$ are shown in table 7.

		α		
		1%	2%	3%
$Q_{a\text{-}1hole}*10^{-8}$ (m^3/s)	Part Load	3.88	7.83	11.87
	BEP	11.08	22.39	33.94
	High Load	12.07	24.38	36.95

***Table 7**- air flow rate from one hole values, depending on void fraction and working point.*

Now that is known the working points and the air flow which is requested, the next step is to find all the device that are needed and run the experiment.

5 Materials and methods

In the previous chapter, a well description about the turbine and the draft tube was taken. This chapter is focalized more on the air injection method, with a description about the devices used for injecting air and measuring the air flow rate.

***Figure 21**- the air injector*.

There are two type of air injectors, one with an injection hole of 1 mm diameter and one with 2 mm injection hole, to verify if the dimension of the hole is irrelevant. Figure 21 shows one of them. On the left there is the air injection section, the black band in the middle shows where is better to fix it with the draft tube to have the injection hole perfectly aligned with the inner wall. On the right there is an on/off switch used to stop the air injection, and to make impossible for the water to go inside the injector when there is no air injection. After that there is a small tube for connect the injector with the pipe to receive the air to inject. Figure 22 shows the injector connected to the draft tube.

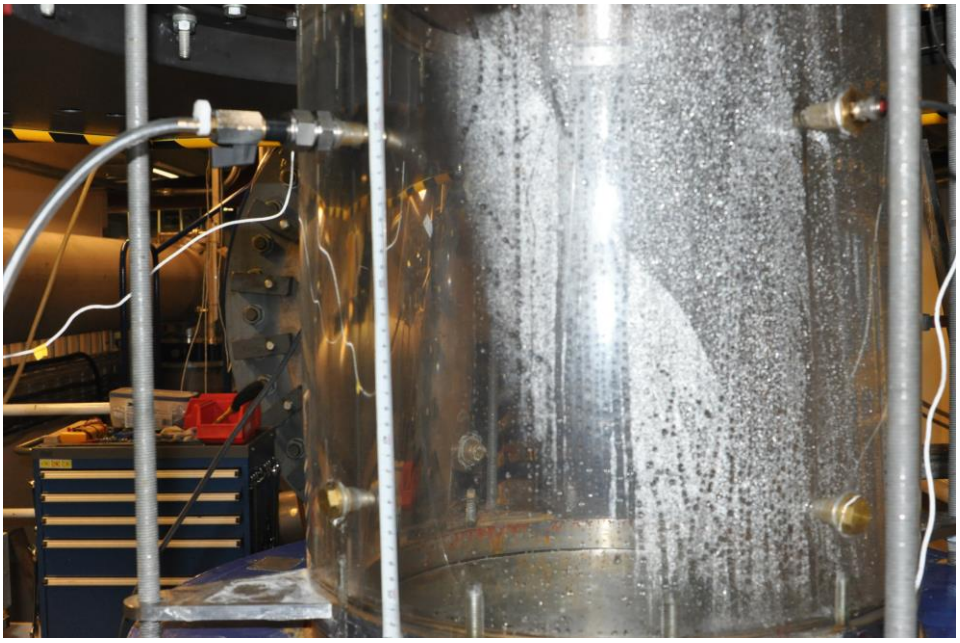

***Figure 22**- the connection between air injector and draft tube.*

From the project "Francis99" [website 6] is possible to find the values of the pressure in the draft tube for every working point. Average values are shown in table 8.

	Part Load	BEP	High Load
P_{in} [bar]	1.014	1.025	1.012

***Table 8**- water pressure values in the draft tube at different working points.*

As might be expected, the pressure values inside the draft tube, even at different working points, are not too far from the value of atmospheric pressure (P_{amb}=1.01325 bar). This is very important in order to know the range of pressure values of air injection, which controls the flow rate.

In the NTNU's Water Power Laboratory there is a pipe in which air flows at a pressure of 7 bar. Figure 23 shows the devices that take the air from

this pipe, make a regulation of the air flow to reached values, and then send it to the injector.

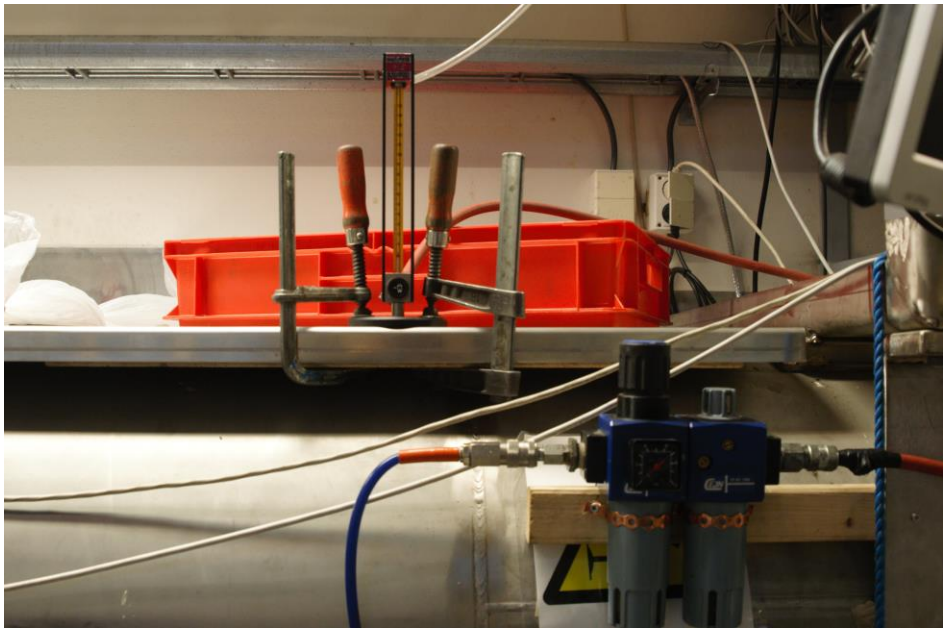

***Figure 23**- the air regulator system.*

The blue pipe connects the 7 bar pressure tube to a pressure regulator, which is connected by the orange pipe to an air flow rate regulator, that is connected by the white pipe to the air injector.

***Figure 24**- the air pressure regulator.*

Figure 24 shows the pressure regulator. To regulate the pressure the black rotatable knob positioned upon the air pressure indicator is used. This

device has an upper permitted pressure of 10 bar and an accuracy of 0.1 bar. It doesn't permit a very fine air pressure regulator, and also it doesn't permit to know the air flow rate. It is only used to regulate pressure from the initial 7 bar to 2 bar, which is closer to the pressure inside the draft tube, that makes easier and better the regulation of the air flow rate by the air flow regulator.

***Figure 25**- the air flow rate regulator*.

Figure 25 shows the air flow rate regulator. It is a "Brooks instrument" from Emerson electric co.. This analogic meter consists in a glass cylinder with a ball of different materials inside, which floats depending on the air flow rate passing through the cylinder, that is regulated by the black rotatable knob positioned at the base of the cylinder. The graduation of the cylinder is from 0mm to 150mm and an accuracy of 1mm. The range of the air flow rate measured depends on the cylinder section and the material of the ball inside it. To choose them, firstly there is a sizing calculations to do, and then a table where the ranges of the air flow rate in standard

conditions (T_{a_std}, P_{a_std} and ρ_{a_std}) are written, that multiplied by the sizing factors give the actual air flow measured. The sizing equation is:

$$\boldsymbol{Sizing\ factor} = \sqrt{\frac{\boldsymbol{\rho_a}}{\boldsymbol{\rho_{a\_std}}} * \frac{\boldsymbol{T_a}}{\boldsymbol{T_{a\_std}}} * \frac{\boldsymbol{P_{a\_std}}}{\boldsymbol{P_a}}}$$

Formula 34

The air is injected in the draft tube, so the operating pressure could be taken equal to the standard pressure. Also the operating temperature is close to 293.1 K. That means that the density is near to the standard density too. The result is that the sizing factor could be taken equal to 1, so the value of maximum air flow in table 9 is the actual one, which means that the chosen cylinder-floating ball combination is the one closest to the maximum values of air injection. That value is given by the high load working points with α=3%, which is 36.95 * 10^{-8} m^3/s (correspond to 1.33 l/h, from table 7).

TUBE	FLOAT	AIR [l/h]
R-2-15-AAA	Glass	2.78
R-2-15-AAA	Sapphire	4.32
R-2-15-AAA	316 SS	8.28
R-2-15-AAA	Carbology	14
R-2-15-AAA	Tantalum	15.3
R-2-15-AA	Glass	5.4
R-2-15-AA	Sapphire	8.2
R-2-15-AA	316 SS	15.9

***Table 9**- maximum air flow rate values measured by the instrument.*

From table 9 the chosen air flow meter is the R-2-15-AAA tube with the glass float, which has a maximum air flow rate of 2.78 l/h, that correspond to the value of 150 mm of the instrument scale. Figure 26 is the air flow calibration curve, which shows the relation from the height of the floating ball and the percent of the maximum air flow rate measured.

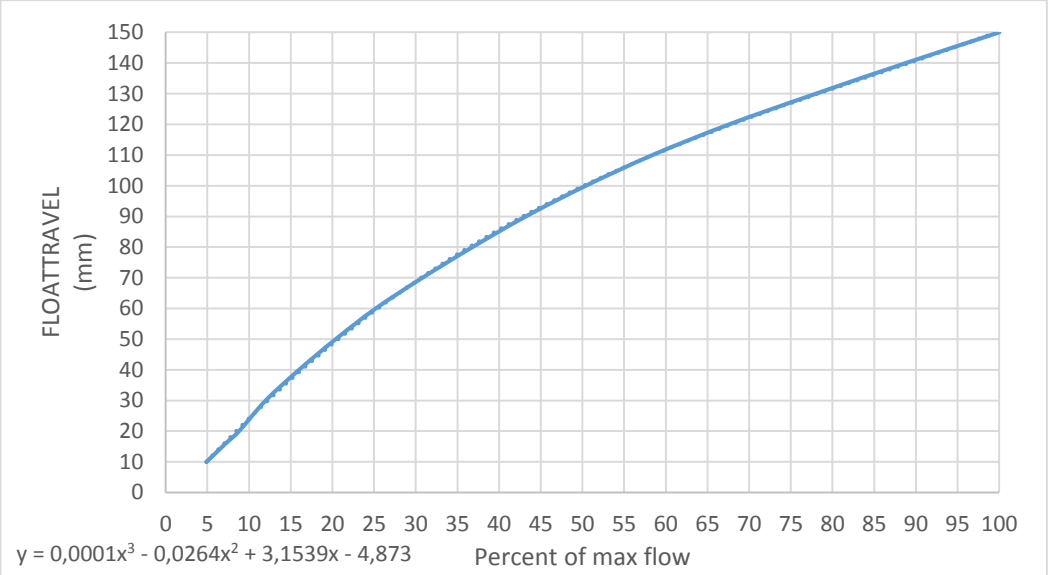

***Figure 26**- air flow calibration curve.*

Under the graphic on the left it is possible to see the interpolation curve function, which describe very well the shape of the curve.

The last device used for this experiment is the camera with which all the photos were taken. The best way to take the photos of the bubbles would be a laser measurer or a film motion analyzer. Unfortunately, in the laboratory this kind of devices was not available. Instead of this, a Nikon digital camera D90 was used (Figure 27), with an EX sigma, 24-70 mm 1:2.8 DG HSM Φ=80 lense.

Figure 27*- camera used in the experiment.*

The problem of using this device is that the picture could not be so accurate, and also it doesn't permit to take photo from the top and the side of the injector at the same time. This means that the values of the diameters measured have to be considered only as an estimation.

6 Results

Now that the experiment is explained and all the devices used are well described, the experience can start. Firstly, the injector with 1mm diameter hole was used, and the turbine ran at best efficiency point, part load and high load. After that, the turbine was stopped and emptied of water, to change the injector with the one with 2 mm diameter hole. After that, the turbine was made run again at best efficiency point, part load and high load. For all the working points, the air flow rate was changed with the air flow regulator, and photos of the bubbles created wer taken. The air flow calibration curve (Figure 26) starts at a values of 10, which is the 5% of the maximum air flow rate (5% of $7.73*10^{-7}$ m^3/s, which is $3.78*10^{-8}$ m^3/s). During the experiment was impossible to start the measure from this point, because the air flow was too low and was impossible to stabilize because of the fluctuations due probably to the fact that the instrument was at the bottom of the scale and as far as the behavior of the turbine is fixed, however, it is subject to small variations. Therefore, for all the working points the pictures of the bubbles were taken for a float travel values from 20 mm to 150 mm, every 10 mm. This is not so good for the aim of this thesis, because the air flow rate needed for assure void fraction of 1%, 2% and 3% from one hole are:

		α		
		1%	2%	3%
$Q_{a\text{-}1hole}*10^{-8}$ (m^3/s)	Part Load	3.88	7.83	11.87
	BEP	11.08	22.39	33.94
	High Load	12.07	24.38	36.95

Table 7*- air flow rate from one hole values, depending on void fraction and working point.*

This means that α=1% of the part load working point has a too small value of air injected, not measurable with that instrument.

***Figure 28**- picture of bubbles created during the experiment*.

Figure 28 showed an example of a picture taken during the experiment. As is possible to see, not all the bubbles has a spherical dimension so is difficult to measure the exact diameter of them. To do that, every picture was put in the AutoCad program, scaling with the dimension of the injector's diameter (11 mm) and then the bubble's diameter was measured. For the bubbles that has not a spherical shape, the diameter was calculate with the formula 35, used in [2]:

$$\boldsymbol{d = 2 * \sqrt{a * b}} \qquad \textbf{Formula 35}$$

Where a and b are the dimensions of the length and the thickness of the bubbles. Not all the pictures taken were good enough to be used because

of the difficulty to focus with the camera both the injector and the bubbles. Also, the scaling method with AutoCad has an error due to the difficulty to take the right borders of the injector. For these reasons, the diameters found has to be consider as an estimate of actual measurement.

6.1 Best Efficiency Point (BEP)

The best efficiency point is the working point where the turbine has the best efficiency, about η=92.61%. In the table below are written all the values of bubble's diameter expected and measured with 1 mm hole injector and 2 mm hole injector. Of course, the value of the water velocity is the same for all the air flow rate, because it only depends on the water flow rate of the working point and the section of the draft tube, which are fixed.

Best efficiency point					
Float Travel	Qa(l/h)	Uw(m/s)	d_exp	dmeas_1mm	dmeas_2mm
20	0,24	2,11	0,43	0,34	0,48
30	0,33	2,11	0,50	0,44	0,51
40	0,44	2,11	0,58	0,53	0,55
50	0,57	2,11	0,66	0,59	0,56
60	0,70	2,11	0,73	0,65	0,68
70	0,86	2,11	0,81	0,70	0,73
80	1,02	2,11	0,88	0,71	0,84
90	1,20	2,11	0,95	0,72	0,93
100	1,40	2,11	1,03	0,79	1,06
110	1,62	2,11	1,11	0,87	1,12
120	1,88	2,11	1,19	0,98	1,17
130	2,17	2,11	1,28	1,13	1,29
140	2,47	2,11	1,37	1,22	1,31
150	2,78	2,11	1,45	1,21	1,27

***Table 10**- bubble's diameters expected and measured with 1 mm and 2 mm hole's diameter, for BEP.*

In that table, d_exp is the expected value of the bubble's diameter from formula 36, dmeas_1mm and dmeas_2mm are the values of the diameter from the picture of the experiment, respectively with 1 mm injector and 2 mm injector.

$$\boldsymbol{d\_exp = d = 2.4 * \left(\frac{Q_{a\_1hole}}{U_w}\right)^{\frac{1}{2}}} \qquad \textbf{Formula 36}$$

Figure 29 is the graphic of the values of diameters measured by the two types of injectors in relation with the diameter expected.

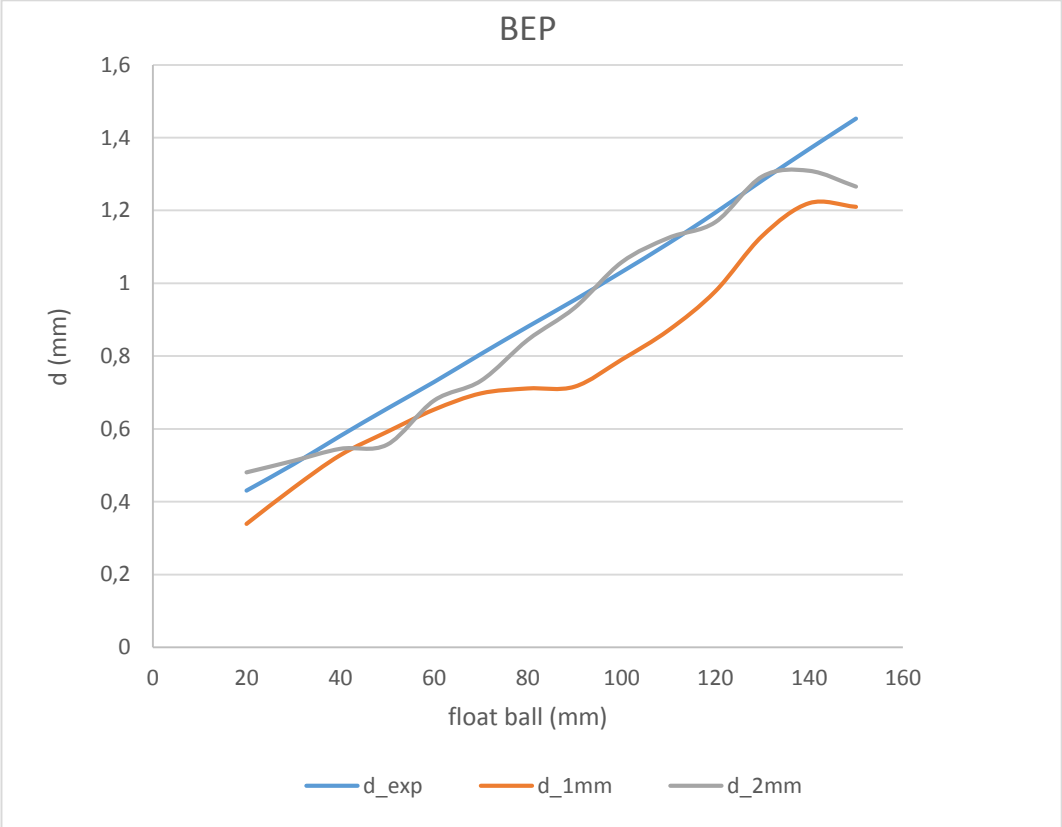

***Figure 29**- trend of the bubbles diameter, for BEP.*

The graphic shows that the 2 mm hole seems to be more accurate than the 1 mm, but considering all the error that could affect the measure, both could be considered very good. Moreover, during the experiment the bubbles were not produced continuously, but the air came out from the injector at intervals that become smaller by increasing the air flow.

Furthermore, the bubbles were very close to the wall for all the length of the plexiglass draft tube.

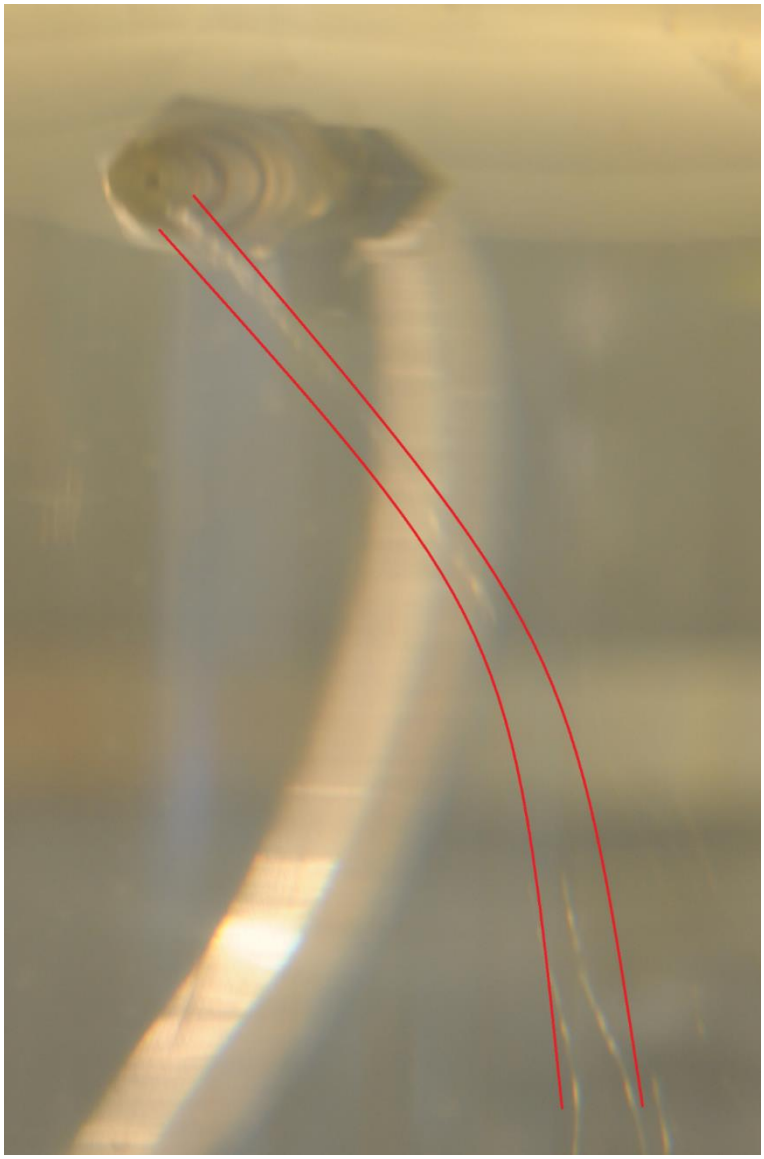

***Figure 30**- direction of bubbles injected in the draft tube, for BEP.*

Figure 30 shows the direction of the bubble's injected. Although the trend does not follow a straight line but follow the rotating fluid vein, due to the rotation of the turbine, the bubbles stay close to the wall all along their way, so there is no reason to think that this bubble's trend will affect the reduction of friction.

6.2 High Load

In the high load working point the efficiency is smaller than the best efficiency point, but the water flow rate is higher, which means that the value of the water velocity is greater. In the table below are written all the values of bubble's diameter expected and measured with 1 mm hole injector and 2 mm hole injector. Of course, the value of the water velocity is the same for all the air flow rate, because it only depends on the water flow rate of the working point and the section of the draft tube, which are fixed.

High load					
Float Travel	Qa(l/h)	Uw(m/s)	d_exp	dmeas_1mm	dmeas_2mm
20	0,24	2,30	0,41	0,67	0,58
30	0,33	2,30	0,48	0,70	0,59
40	0,44	2,30	0,56	0,71	0,63
50	0,57	2,30	0,63	0,72	0,63
60	0,70	2,30	0,70	0,75	0,76
70	0,86	2,30	0,77	0,72	0,78
80	1,02	2,30	0,84	0,82	0,85
90	1,20	2,30	0,91	1,05	0,91
100	1,40	2,30	0,99	1,07	1,02
110	1,62	2,30	1,06	1,08	1,13
120	1,88	2,30	1,14	1,14	1,29
130	2,17	2,30	1,23	1,31	1,41
140	2,47	2,30	1,31	1,34	1,43
150	2,78	2,30	1,39	1,27	1,40

***Table 11**- bubble's diameters expected and measured with 1 mm and 2 mm hole's diameter, for high load.*

In that table, d_exp is the expected value of the bubble's diameter from formula 36, dmeas_1mm and dmeas_2mm are the values of the diameter from the picture of the experiment, respectively with 1 mm injector and 2 mm injector.

$$\boldsymbol{d\_exp = d = 2.4 * \left(\frac{Q_{a\_1hole}}{U_w}\right)^{\frac{1}{2}}} \qquad \textbf{Formula 36}$$

Figure 31 is the graphic of the values of diameters measured by the two types of injectors in relation with the diameter expected.

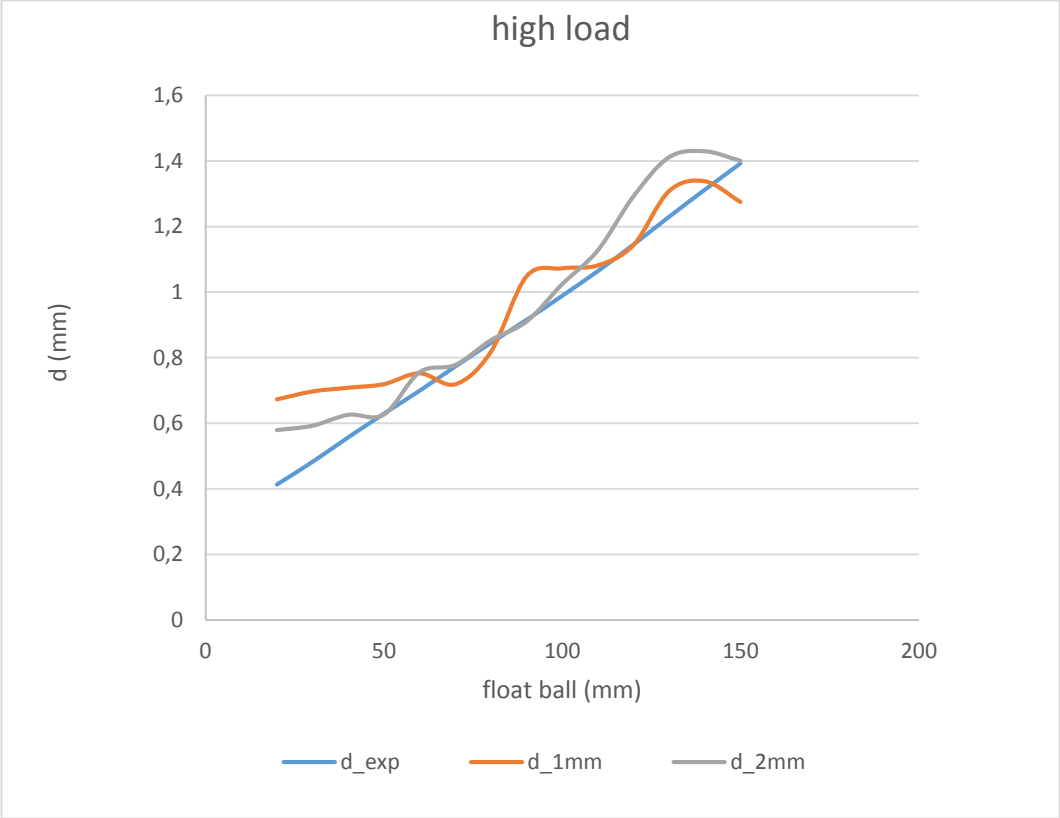

***Figure 31**- trend of the bubbles diameter, for high load.*

The graphic shows that the 2 mm hole seems to be more accurate than the 1 mm, and both the measured values are so far from the expected value in the first part with low air injection, but considering all the error that could affect the measure, both could be considered very good. Moreover, during the experiment the bubbles were not produced continuously, but the air

came out from the injector at intervals that become smaller by increasing the air flow. These intervals are greater than the one with same air flow rate of the best efficiency point, which means that they depend also on the water flow rate. Furthermore, the bubbles were very close to the wall for all the length of the plexiglass draft tube.

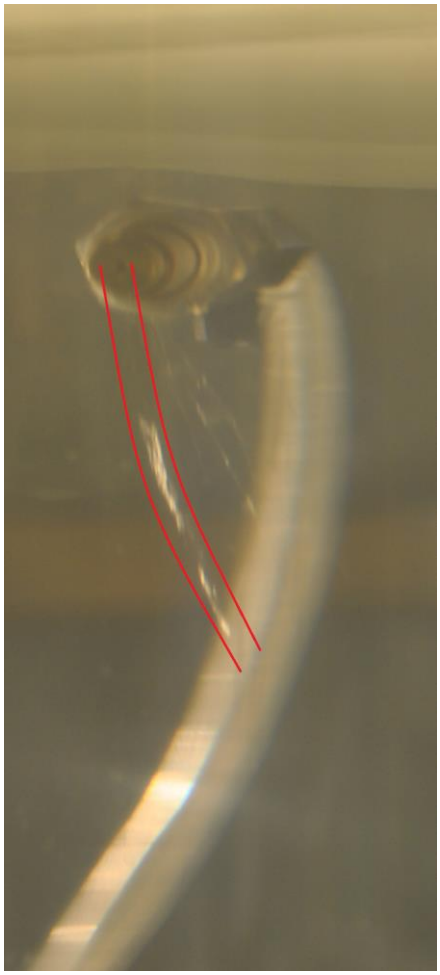

***Figure 32**- direction of bubbles injected in the draft tube, for high load.*

Figure 32 shows the direction of the bubble's injected. The trend does not follow a straight line but follow the rotating fluid vein due to the turbine rotation, and it is more linear than the BEP one, which suggests that the more is the water flow rate, more linear is the direction of the bubbles. Also in this case bubbles always stay close to the wall, so there is no reason to think that this trend of the bubble will affect the reduction of friction.

6.3 Part Load

This working point has less efficiency than the others and also less water flow rate, which means that the velocity of the water is smaller and the bubble's diameter greater than the other points. In the table below are written all the values of bubble's diameter expected and measured with 1 mm hole injector and 2 mm hole injector. Of course, the value of the water velocity is the same for all the air flow rate, because it only depends on the water flow rate of the working point and the section of the draft tube, which are fixed.

Part load					
Float Travel	Qa(l/h)	Uw(m/s)	d_exp	dmeas_1mm	dmeas_2mm
20	0,24	0,74	0,73	0,57	0,85
30	0,33	0,74	0,85	0,58	0,79
40	0,44	0,74	0,98	0,66	0,87
50	0,57	0,74	1,11	0,67	0,90
60	0,70	0,74	1,23	0,84	1,16
70	0,86	0,74	1,36	0,76	1,30
80	1,02	0,74	1,49	0,92	1,34
90	1,20	0,74	1,61	0,93	1,46
100	1,40	0,74	1,74	1,12	1,72
110	1,62	0,74	1,88	1,22	1,85
120	1,88	0,74	2,02	1,41	1,99
130	2,17	0,74	2,17	1,55	2,29
140	2,47	0,74	2,31	1,73	2,18
150	2,78	0,74	2,46	1,80	2,47

***Table 12**- bubble's diameters expected and measured with 1 mm and 2 mm hole's diameter, for part load.*

In that table, d_exp is the expected value of the bubble's diameter from formula 36, dmeas_1mm and dmeas_2mm are the values of the diameter from the picture of the experiment, respectively with 1 mm injector and 2 mm injector.

$$\boldsymbol{d\_exp = d = 2.4 * \left(\frac{Q_{a\_1hole}}{U_w}\right)^{\frac{1}{2}}} \qquad \textbf{Formula 36}$$

Figure 33 is the graphic of the values of diameters measured by the two types of injectors in relation with the diameter expected.

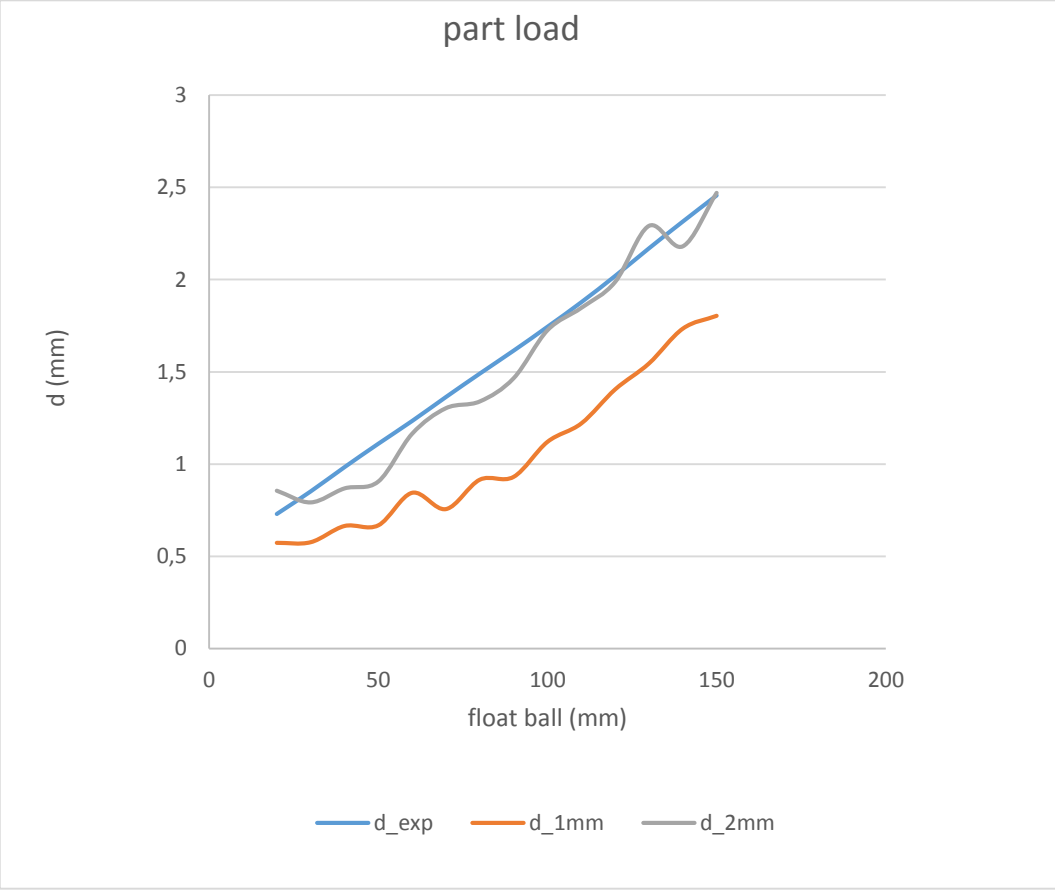

***Figure 33**- trend of the bubbles diameter, for part load.*

The graphic shows that the 2 mm hole seems to be more accurate than the 1 mm, and the 1 mm values are smaller than the expected and the 2 mm values, but considering all the error that could affect the measure, also these measures could be considered very good. Like the other two cases,

during the experiment the bubbles were not produced continuously, but the air came out from the injector at intervals that become smaller by increasing the air flow. Unlike the case of high load, in this case the intervals was smaller than the one with same air flow rate of the best efficiency point, which means that the length of the intervals is direct proportional to the water flow rate value. Furthermore, the bubbles were very close to the wall but not for all the length of the plexiglass draft tube. Due to the rotation of the water and the smaller velocity respect the cases of best efficiency point and high load, the bubbles moved away from the wall of the draft tube to the center of the water flow rate. Figure 34 shows this phenomenon, that cause a vortex of air bubbles in the middle of the draft tube, highlighted by the red lines in the picture, which became stronger depending on how much air is injected.

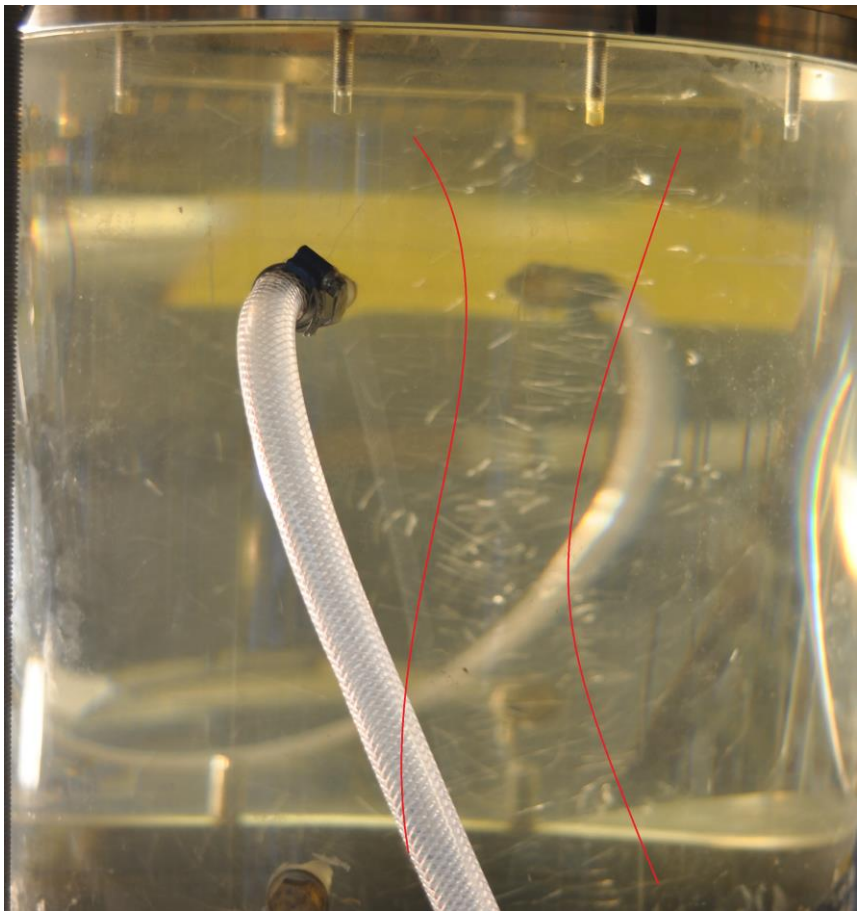

Figure 34- *air vortex in the middle of the draft tube, for part load.*

Due to this vortex, it was impossible to take a photo good enough of the trend of the bubbles going out from the injectors, because it was too complicated distinguishing bubbles of the vortex from bubbles that goes out from the injector, as it is shown in figure 35.

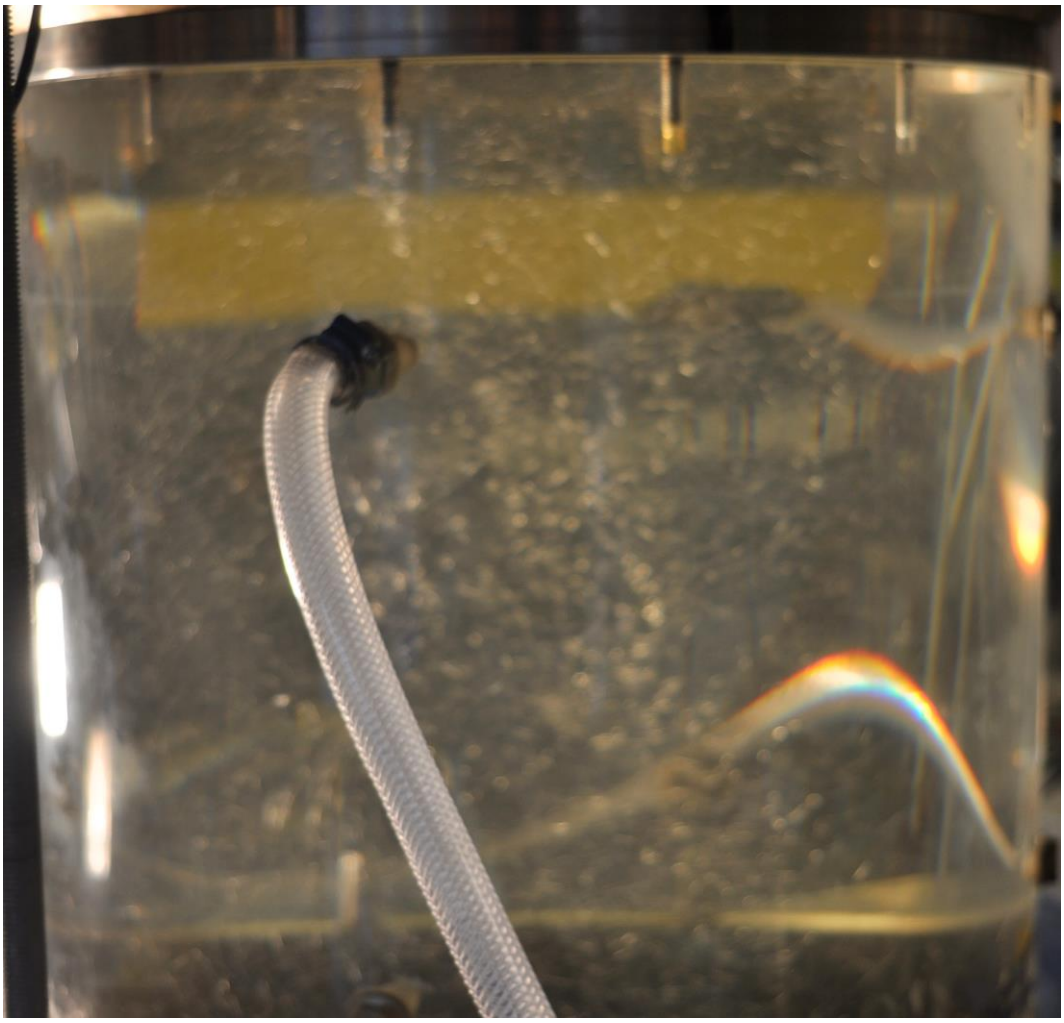

Figure 35*- bubbles in the middle of the draft tube, for part load.*

Also if it is impossible to see in the picture, in this case the trend of the bubbles going out from injector follow the rotating fluid vein more than the best efficiency point case, which means that more is the water flow rate, more the trend of the bubbles is a vertical straight line.

7 Conclusions and possible future works

The skin friction reduction using air injection is a great way to reduce the friction between a moving liquid and the wall where the liquid flows. The first part of this thesis is focalized on a way to use this method in a draft tube of a Francis turbine, reducing the pressure losses to improve the energy creates by the turbine. To do that, from the literature review are obtained the right values of air to be injected and the characteristics that the air bubbles must have to ensure a reduction of friction. The solution is a ring with 18500 holes placed between the turbine and the draft tube, which with the right amount of air injected should ensure a void factor of 1%, 2% and 3%, which, from the literature review, should be enough to have a good friction reduction.

Unfortunately was not possible verified if this method works in the laboratory, so the experiment was changed in the behavior of the bubbles when injected in the draft tube of a Francis turbine. In the experiment, three different working points of the turbine were proved, which are best efficiency point, part load and high load, with different air flow injected and different dimension of the hole of the injector, one with 1 mm diameter and the other with 2 mm diameter. Regarding the different diameters of the injectors, as expected, significant differences regarding the size of the bubbles created are not found, which means that the size of the injector's hole does not affect the dimension of the bubbles.

Concerning the dimension of the bubbles, also if the method used to measure the diameter was not so accurate, a good relation with the formula 21 is obtained.

$$\boldsymbol{d = 2.4 * \left(\frac{Q_a}{U_w}\right)^{\frac{1}{2}}} \qquad \textbf{Formula 21}$$

Another important aspect that comes out from the experiment is that the bubbles were injected not continuously, and the length of the interval from one injection to another depends on the air flow rate (Greater the air flow, less the waiting time) and also on the water flow rate (Greater the water flow, greater the time to wait), but in a less marked way.

Regarding the bubbles in the draft tube, they didn't make a straight line, but a curve due to the water which goes out from the turbine. The trend of the bubbles becomes more linear as the water flow increase.

The water flow rate controls also the time and the space bubbles stay close to the wall: greater is the water flow rate, greater is the time and the space bubbles remain close to the wall. That's the reason why in the part load working point, which is the one with the smallest water flow rate, bubbles are driven from the wall to the center of the draft tube, forming a vortex.

All these results make good expectations about the use of air injection for skin friction reduction in the draft tube.

Regarding future studies and work that could be done, would be very interested to test the ring with 18500 holes to discover if could realize skin friction reduction, to see if the turbine produce more energy. Another aspect that could be study more, is the possibility to improve the dissolved oxygen in the water, and how much could be improved. Furthermore, the air in the draft tube could limit the surging phenomenon, that could also break the turbine.

References

[1] Victor S. L'vov, Anna Pomyalov, Itamar Procaccia, Vasil Tiberkevich, 2005, "Drag reduction by microbubbles in turbulent flows: the limit of minute bubbles"

[2] Hiroharu Kato, Kento Miura, Hajime Yamaguchi, Masaru Miyanaga, 1998, "Experimental study on microbubble ejection method for frictional drag reduction"

[3] Yasuhiro Moriguchi, Hiroharu Kato, 2002, "Influence of microbubble diameter and distribution on frictional resistance reduction"

[4] Steven L. Ceccio, 2010, "Friction drag reduction of external flows with bubble and gas injection"

[5] Xiaochum Shen, Steven L. Ceccio, Marc Perlin, 2006, "Influence of bubble size on micro-bubble drag reduction"

[6] Robert Latorre, Aaron Miller, Richard Philips, 2003, "Micro-bubble resistance reduction on a model SES catamaran"

[7] Brian R. Elbing, Eric, S. Winkel, Keary A. Lay, Steven L. Ceccio, David R. Dowling, Marc Perlin, 2008, "Bubble-induced skin-friction drag reduction and the abrupt transition to air-layer drag reduction"

[8] Yoshiaki Kodama, Akira Kakugawa, Takahito Takahashi, Hideki Kawashima, 2000, "Experimental study on microbubbles and their applicability to ships for skin friction reduction"

[9] Madan Mohan Guin, Hiroharu Kato, Hajime Yamaguchi, Masatsugu Maeda, Masaru Miyanaga, 1996, "Reduction of skin friction by microbubbles and its relation with near-wall bubble concentration in a channel"

[10] Wendy C. Sanders, Eric S. Winkel, David R. Dowling, Marc Perlin, Steven L. Ceccio, 2005, “Bubble friction drag reduction in a high-Reynolds-number flat-plate turbulent boundary layer”

[11] N. M. Nouri, A. Sarreshtehdari, 2009, “Effect of Air Bubble Injection on the Flow Near a Rotary Device”

[12] Thomas H. van den Berg, Dennis P. M. van Gils, Daniel P. Lathrop, Detlef Lohse, 2007, “Bubbly Turbulent Drag Reduction Is a Boundary Layer Effect”

[13] Florentina Bunea, Gabriel D. Ciocan, Gabriela Oprina, Gheorghe Baran, Corina A. Babutanu, 2010, “Hydropower impact on water quality”

[14] Florentina Bunea, Gabriela Osprina, Gabriel D. Ciocan, Gheorghe Baran, Cristinel Ilie, Irina Pincovschi, 2010, “Aeration parameters optimization for an imposed energy consumption”

[15] Benoit Papillon, Michel Sabourin, Michel Couston, Claire Deschenes, 2002, “Methods for air admission in hydroturbines”

[16] Principia Research Corporation, 2008, “Turbine performance and air admission tests”

[17] Koichi Nakanishi, Tsuneo Ueda, 1964, “Air supply into draft tube of Francis turbine”

Websites references

1) http://www.renewableenergyworld.com/rea/tech/hydropower

2) http://www.hydropower.org/

3)http://www.worldenergy.org/data/resources/resource/hydropower/

4)http://www.conserve-energy-future.com/Advantages_HydroPower.php

5)http://nptel.ac.in/courses/112104117/chapter_7/7_7.html

6)http://www.ltu.se/research/subjects/Stromningslara/Konferenser/Francis-99/Test-Case-1.111520?l=en

7) http://www.energoclub.it/doceboCms/page/20/idroelettrico_impatto_ambientale.html

8) http://bcn.boulder.co.us/basin/data/NEW/info/DO.html

Appendix A

This appendix contains one drawing of the draft tube used for the experiment, which is situated in the NTNU water laboratory.

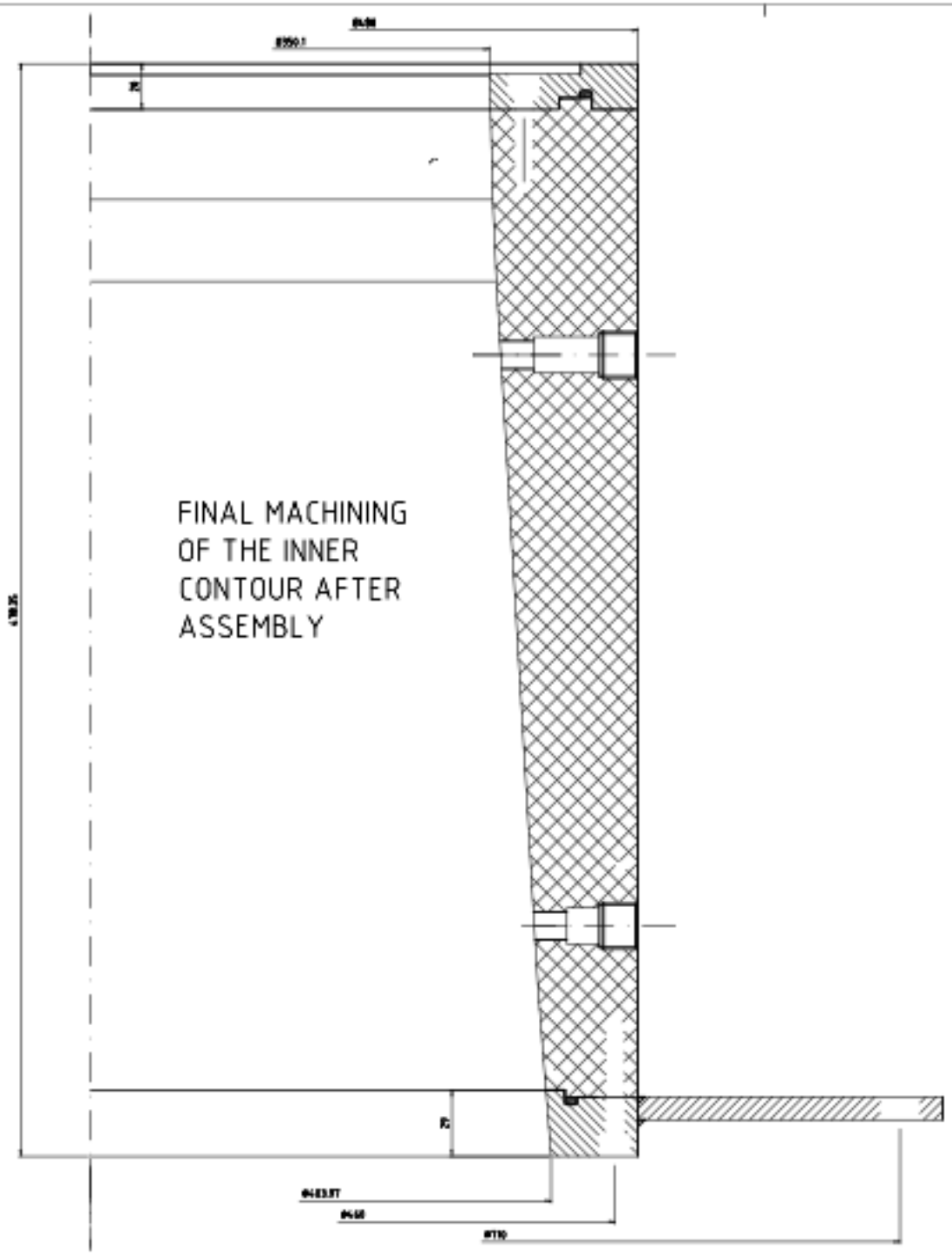

1	7	RUBBER PACKING, [illegible]			RUBBER
12	6	[illegible]			STAINLESS STEEL
1	5	LOWER DRAFT TUBE CONE RING		[illegible]	[illegible]
12	4	[illegible]			STAINLESS STEEL
1	3	RUBBER PACKING, [illegible]			RUBBER
1	2	DRAFT TUBE CONE		[illegible]	ACRYLIC GLASS
1	1	UPPER DRAFT TUBE CONE RING		[illegible]	[illegible]

Model Turbine / Tidal Power Plant		JAT	1:1		NTNU KAVITASJONSLABORATORIET
		BID			
		DRAFT TUBE CONE Assembly			[illegible]
					A3

Appendix B

This appendix contains one drawing of the constitutive part of the draft tube, which are particular of the ring between the turbine and the draft tube and the plexiglass draft tube measure.

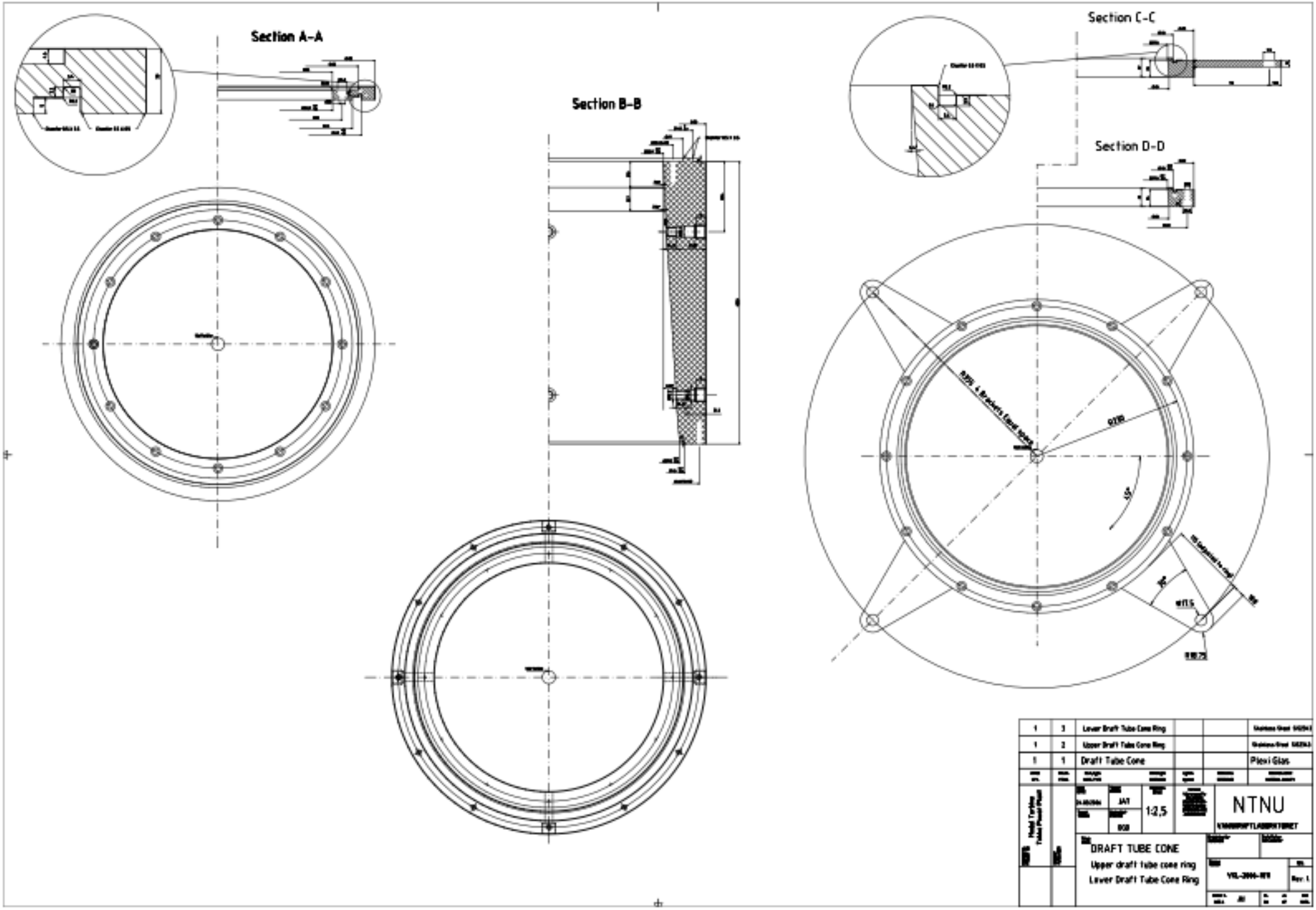
Section A-A
Section B-B
Section C-C
Section D-D
1 3 Lower Draft Tube Cone Ring
1 2 Upper Draft Tube Cone Ring
1 1 Draft Tube Cone Plexi Glas
JAT
1:2,5
908
NTNU
DRAFT TUBE CONE
Upper draft tube cone ring
Lower Draft Tube Cone Ring
VKL-3000-RR
Rev. 1

Appendix C

This appendix contains the manual of the air flow rate meter, in which are showed the various types with their flow of reference and operative characteristics.

Data Sheet
DS-VA-1350-eng
January, 2005

Model GT 1350/1355/1357

Sho-Rate Purgemeter

DESIGN FEATURES

- Simple but rugged construction for easy flow indication
- Integral needle valves for process control
- Integral flow controllers to compensate for varying inlet and/or outlet pressures
- Tubes can be changed in line minimizing process down time
- Kynar construction option for corrosive fluids
- Interchangeable tubes and floats

Model GT 1350/1355 with Needle Valve on Inlet

DESCRIPTION

The Sho-Rate series of flow indicators provide an economical means of flow rate indication and control for general plant use, laboratory and analytical applications. The instruments are ideal for common applications like purging services, cooling water flow indication, bearing lubrication, carrier gas flow rate indication, fuel flow indication in chromatography and atomic absorption and indication and control of doping gas in electronic crystal growing furnaces.

SPECIFICATIONS

Performance

Scale length	**model 1350**	65 mm
	model 1355	150 mm
	model 1357	250 mm
Accuracy	**model 1350**	± 10% F.S.
	Optional	± 5% F.S.
	model 1355	± 5% F.S.
	Optional	± 2% F.S.
	model 1357	± 3% F.S.
	Optional	± 2% F.S.
	or	± 1% F.S.
Repeatability	± 0.5%	
Rangeability	10:1	
Maximum operating pressure	1400 kPa (14 bar)	
Maximum operating temperature	120 °C	
Certified	Intrinsically safe according to ATEX (PTB 99ATEX2128 X) Pressure Equipment Directive (PED) 97/23/EC. Flow meter complies under Sound Engineering Practices (SEP).	

Construction data

Fitting material	Brass or 316 SS
Connection material	Brass or 316 SS
Connection types	• Standard $^1/_8$" NPT • Optional: $^1/_4$" NPT $^1/_8$" tube compression $^1/_4$" tube compression $^1/_4$" I.D. Hose
Side plate material	Anodized aluminium
Metering tube material	Borosilicate glass
Float material	Pyrex, Sapphire, 316 SS, Carboloy or Tantalum
Float stop material	Teflon
Tube packing material	Viton
O-Ring material	Viton

Capacity Table Model 1350

TUBE	FLOAT	MODEL CODE	l_n/h AIR	l/h H_2O	DECAL** l_n/h AIR*	DECAL** SCFH AIR*	DECAL** l/h H_2O	DECAL** GPH H_2O
R-2-65-5	Glass	A1	4.29	-	0.4-4.2	0.01-0.16	-	-
R-2-65-5	316 SS	A3	13.5	-	1.5-13.5	0.02-0.52	-	-
R-2-65-5	Carboloy	A4	22	-	2-22	0.04-0.85	-	-
1-65	Glass	B1	42	0.60	4-42	0.2-1.2	0.04-0.6	0.01-0.14
2-65A	Glass	C1	50	-	6-50	0.4-2.0	-	-
2-65B	316 SS	D3	165	4.68	15-165	0.5-5.0	0.4-4.6	0.1-1.0
2-65C	316 SS	E3	-	2.38	-	-	0.2-2.3	0.05-0.5
3-65	Glass	F1	180	3.6	15-180	0.5-6.0	0.3-3.6	0.05-0.7
3-65	316 SS	F3	319	7.9	30-310	1.0-10	0.6-7.8	0.1-1.6
4-65	Glass	G1	359	8.8	30-350	1.2-12	0.8-8.8	0.2-2.0
4-65	316 SS	G3	628	22.1	60-620	2.0-18	2-22	0.5-4.0
6-65	Glass	H1	1297	37.0	150-1300	5.0-50	3-37	1.0-11
6-65	316 SS	H3	2341	77.1	200-2300	10-90	6-76	2.0-20
6-65	Carboloy	H4	3500	109	300-3500	12-120	10-105	2.0-30

* Flow is given at normal conditions (0 °C & 1.013 bar absolute) when the meter is operated at 20 °C & 1.013 bar absolute

** In case the instruments are supplied with a direct reading decal fused on the tube, the flow range values stated in these columns must be used

Capacity Table Model 1355

TUBE	FLOAT	MODEL CODE	l_n/h AIR	l/h H_2O
R-2-15-AAA	Glass	A1	2.78	0.033
R-2-15-AAA	Sapphire	A2	4.32	0.064
R-2-15-AAA	316 SS	A3	8.28	0.15
R-2-15-AAA	Carboloy	A4	14	0.296
R-2-15-AAA	Tantalum	A5	15.3	0.33
R-2-15-AA	Glass	B1	5.4	0.033
R-2-15-AA	Sapphire	B2	8.2	0.125
R-2-15-AA	316 SS	B3	15.9	0.315
R-2-15-AA	Carboloy	B4	26.9	0.575
R-2-15-AA	Tantalum	B5	29.1	0.670
R-2-15-D	Glass	F1	21	0.34
R-2-15-D	Sapphire	F2	29	0.63
R-2-15-D	316 SS	F3	46	1.35
R-2-15-D	Carboloy	F4	69	2.09
R-2-15-D	Tantalum	F5	73	2.26
R-2-15-A	Glass	C1	46	1.00
R-2-15-A	Sapphire	C2	61	1.57
R-2-15-A	316 SS	C3	94	2.76
R-2-15-A	Carboloy	C4	136	4.24
R-2-15-A	Tantalum	C5	144	4.54
R-2-15-B	Glass	D1	133	3.2
R-2-15-B	Sapphire	D2	173	4.8
R-2-15-B	316 SS	D3	262	7.9
R-2-15-B	Carboloy	D4	376	12.1
R-2-15-B	Tantalum	D5	398	13.1
R-2-15-C	Glass	E1	221	5.2
R-2-15-C	Sapphire	E2	292	8.0
R-2-15-C	316 SS	E3	439	13.3
R-2-15-C	Carboloy	E4	629	20.3
R-2-15-C	Tantalum	E5	667	21.9
R-6-15-A	Glass	G1	510	12.3
R-6-15-A	Sapphire	G2	669	18.3
R-6-15-A	316 SS	G3	944	30.0
R-6-15-A	Carboloy	G4	1347	44.4
R-6-15-A	Tantalum	G5	1430	47.7
R-6-15-B	Glass	H1	1296	34
R-6-15-B	Sapphire	H2	1690	49
R-6-15-B	316 SS	H3	2500	80
R-6-15-B	Carboloy	H4	3549	117
R-6-15-B	Tantalum	H5	3644	125

Capacity Table Model 1357

TUBE	FLOAT	MODEL CODE	ln/h AIR*	l/h H2O
R-2-25-D	Glass	D1	20	0.33
R-2-25-D	Sapphire	D2	28	0.61
R-2-25-D	316 SS	D3	45	1.21
R-2-25-D	Carboloy	D4	67	1.94
R-2-25-D	Tantalum	D5	71	2.10
R-2-25-A	Glass	A1	47	1.0
R-2-25-A	Sapphire	A2	62	1.6
R-2-25-A	316 SS	A3	96	2.8
R-2-25-A	Carboloy	A4	138	4.3
R-2-25-A	Tantalum	A5	147	4.6
R-2-25-B	Glass	B1	123	2.9
R-2-25-B	Sapphire	B2	160	4.5
R-2-25-B	316 SS	B3	242	7.4
R-2-25-B	Carboloy	B4	347	11.1
R-2-25-B	Tantalum	B5	370	11.9
R-2-25-C	Glass	C1	212	4.9
R-2-25-C	Sapphire	C2	277	7.5
R-2-25-C	316 SS	C3	416	12.8
R-2-25-C	Carboloy	C4	579	19.1
R-2-25-C	Tantalum	C5	611	20.5
R-6-25-A	Glass	E1	483	11.8
R-6-25-A	Sapphire	E2	619	17.6
R-6-25-A	316 SS	E3	910	29.2
R-6-25-A	Carboloy	E4	1280	43.0
R-6-25-A	Tantalum	E5	1356	45.8
R-6-25-B	Glass	F1	1273	33
R-6-25-B	Sapphire	F2	1621	49
R-6-25-B	316 SS	F3	2349	80
R-6-25-B	Carboloy	F4	3283	113
R-6-25-B	Tantalum	F5	3470	120

ALARM CONTACTS

• Inductive bistable ring initiators for high and/or low flow alarm may be mounted to the instrument to create a highly sensitive, stable and accurate device for signalling high or low flows or deviations from a controlled flow. The inductive alarm, (⟨Ex⟩ II2G EEx ia IIC T6) can only be used in combination with 316 SS or carboloy ball floats and only with scales on tube. The alarm points may be adjusted over the entire flow meter range and be set so that any two contacts may be made to operate simultaneously. For hazardous area applications Brooks can supply an ATEX approved (Eex) ia IIC power supply/amplifier/relay unit to obtain an intrinsic safe current circuit.

DIMENSIONAL DRAWINGS

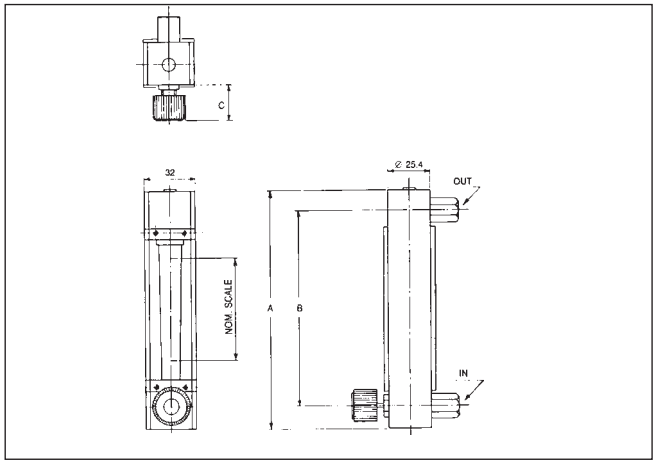

MODEL	CONNECTIONS	A	B	C
1350	1/8" NPT	140	114	26
1355	1/8" NPT	249	224	26
1357	1/8" NPT	376	351	26

OPTIONAL FEATURES/EQUIPMENT

• Kynar fitting material

The kynar (P.V.D.F.) fitting material provides an economical means of flow rate indication for difficult to handle, corrosive fluids encountered in chemical plants, research laboratories, semiconductor and film processing industries.

• Standard Valve or ELF Needle Valve

The Standard Valve is a multi-purpose valve.
The ELF Needle Valve (Non Rising Stem design) provides a greater number of turns affording greater precision control with higher resolution. Both valves provide positive shut-off and both are directly interchangeable. Both valves can be installed at the inlet or the outlet fitting of the flowmeter.

• Panel Mounting Arrangements

Flush mounting bezel

The instrument can be equipped with an aluminium (model 1350 and 1355) or plastic (model 1357) bezel for flush panel mounting.

Threaded adapters with mounting nuts for front panel mounting (See drawing below)

• Integrally mounted flow controllers

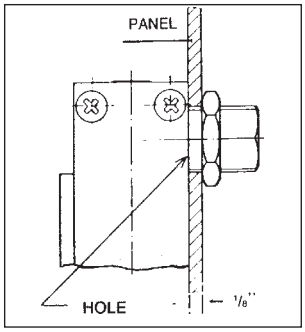

Brooks self-contained flow controllers are constant differential regulators with built-in flow control needle valve. The internal diaphragm-actuated control valve is positioned by the incoming fluid pressure on one side of the diaphragm, and outlet pressure + spring action on the other side. Variations in the supply and/or discharge pressure, disturb the balance of forces on the diaphragm, causing the control valve to close or to open, thus maintaining a fixed differential across the manual flow regulating valve. The series 8800 controllers are designed for all liquid and gas flows with constant downstream pressure. Series 8900 controllers are designed for all liquids and gas flows with constant upstream pressure.
The 8800/8900 controllers are designed to offer an economical way of controlling all your liquid and gas flows.
The 8840/8940 controllers are designed to offer the most accurate way of controlling all your liquid and gas flows.

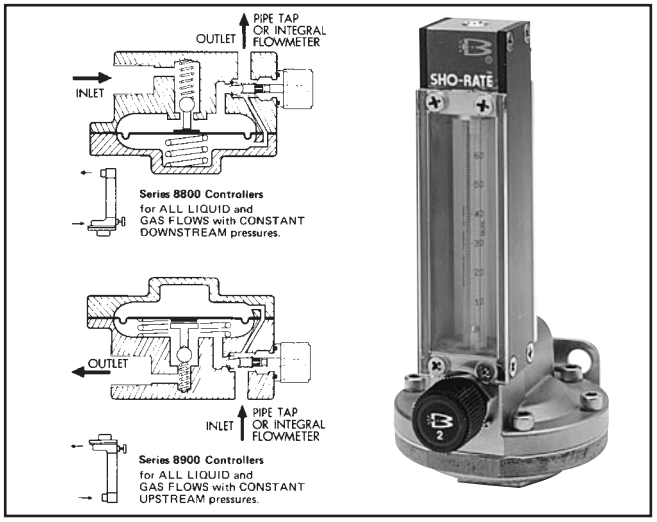

- Inductive switches for high and low flow alarm. One or more inductive sensing coils may be mounted to the instrument to create a highly sensitive, stable and accurate device for signalling high or low flows or deviations from a controlled flow (only for use with 316 SS or Carboloy ball floats).
- In-line sintered metal filter.
- Circular or triangle base plates with screws and spirit level.
- Multi-tube construction with manifold or individual inlet/outlet.

Example Dimensional Drawing Multi-Tube Sho-Rate

No of Tube	A
2T	50.8
3T	76.2
4T	101.6
5T	127
6T	152.4

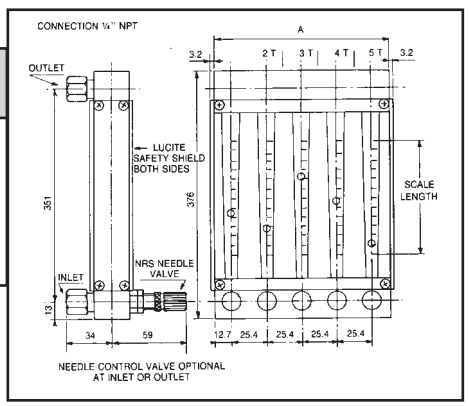

ORDERING INFORMATION

BASE MODEL NUMBER	DESCRIPTION
1350/D	SHO-RATE '65'
1355/D	SHO-RATE '150'
1357/D	SHO-RATE '250'
	FITTING / O-RING MATERIAL
1	BRASS FITTINGS/VITON O-RINGS
2	316 SS FITTINGS/VITON O-RINGS
	TUBE TYPE
X	TO BE SELECTED FROM CAPACITY TABLE
	FLOAT MATERIAL
X	TO BE SELECTED FROM CAPACITY TABLE
	SCALE TYPE
A	MM DECAL + CALIBRATION CURVE
D	DIRECT READING SCALE (NOT WITH ALARM)
E	DIRECT READING DECAL (ln/h AIR @ 20 ∞C & 1,013 BAR ABS)
F	DIRECT READING DECAL (l/h WATER)
G	DIRECT READING DECAL (SCFH AIR @ 70 ∞F & 14,7psig)
H	DIRECT READING DECAL (GPH WATER)
	ACCURACY
	MODEL 1350 MODEL 1355 MODEL 1357
1	± 10 % F.S. ± 5% F.S. ± 3% F.S.
2	± 5 % F.S. ± 2% F.S. ± 2% F.S.
3	± 1% F.S.
	CONNECTIONS
A	1/8" NPT FEMALE (NOT WITH FLOW CONTROLLER)
B	1/4" NPT FEMALE (ST'D WITH FLOW CONTROLLER)
C	1/8" TUBE COMPRESSION
D	1/4" TUBE COMPRESSION
E	1/4" I.D.HOSE
	FLOW CONTROLLER/NEEDLE VALVE
0	NONE
1	8800 FLOW CONTROLLER
2	8900 FLOW CONTROLLER
3	8840 FLOW CONTROLLER
4	8940 FLOW CONTROLLER
5	VALVE POSITIONED AT INLET SIDE
6	VALVE POSITIONED AT OUTLET SIDE
	VALVE SIZE
0	NONE
A	STANDARD VALVE # 1
B	STANDARD VALVE # 2
C	STANDARD VALVE # 3
D	NRS NEEDLE VALVE # 1
E	NRS NEEDLE VALVE # 2
F	NRS NEEDLE VALVE # 3
G	NRS NEEDLE VALVE # 4
H	NRS NEEDLE VALVE # 5
J	NRS NEEDLE VALVE # 6
K	NRS NEEDLE VALVE # 7
	BISTABLE ALARM
0	NONE
A	1 LIMIT SENSOR
B	2 LIMIT SENSORS
C	1 LIMIT SENSOR+ I.S. RELAY, 230/110VAC KFA6/KFA5-SR2-Ex1.W
D	2 LIMIT SENSORS+ I.S. DOUBLE RELAY, 230/110Vac KFA6/KFA5-SR2-Ex2.W
	MOUNTING
0	NONE
1	ALUMINIUM BEZEL
2	THREADED ADAPTERS (NPT ONLY) WITH PANEL MOUNTING NUTS
3	MOUNTING BRACKET FOR CONTROLLER
4	CIRCULAR BASEPLATE (ALUMINIUM)
9	SELECT "9" OR "Z" IF SPECIAL AND SPECIFY
1350 / D 2 A 1 A 1 A 5 D A 1 = TYPICAL MODEL NUMBER	

ISO 9001
QUALITY SYSTEM
Certificate of Conformity
The Quality System at Brooks Instrument conforms to the quality standards set forth in ISO 9001.

Emerson Process Management
Brooks Instrument
407 West Vine Street
P.O.Box 903
Hatfield, PA 19440-0903 USA
T (215) 362-3700
F (215) 362-3745
E-Mail BrooksAm@EmersonProcess.com
www.EmersonProcess.com/BrooksInstrument

Emerson Process Management
Brooks Instrument B.V.
Neonstraat 3
P.O. Box 428
6710 BK Ede, Netherlands
T 31-318-549-300
F 31-318-549-309
E-Mail BrooksEu@EmersonProcess.com

Emerson Japan, Ltd.
Emerson Process Management
Brooks Instrument
1-4-4 Kitasuna Koto-Ku
Tokyo, 136-0073 Japan
T 011-81-3-5633-7105
F 011-81-3-5633-7124
E-Mail BrooksAs@EmersonProcess.com

EMERSON
Process Management